Title

PREPARATION AND CHARACTERIZATION OF NOVEL BORON NITRIDE INTERCALATION COMPOUNDS AND AG (III) FLUOROCOMPLEXES

Author

Mayorga, S.G.

Publication Date

1988-10-01

Thesis/dissertation

Lawrence Berkeley Laboratory
UNIVERSITY OF CALIFORNIA

Materials & Chemical Sciences Division

Preparation and Characterization of Novel Boron Nitride Intercalation Compounds and Ag (III) Fluorocomplexes

S.G. Mayorga
(Ph.D. Thesis)

October 1988

Prepared for the U.S. Department of Energy under Contract Number DE-AC03-76SF00098.

DISCLAIMER

PREPARATION AND CHARACTERIZATION OF NOVEL BORON NITRIDE INTERCALATION COMPOUNDS AND Ag (III) FLUOROCOMPLEXES

Steven G. Mayorga

Ph.D. Thesis

Department of Chemistry
University of California

and

Materials and Chemical Science Division
Lawrence Berkeley Laboratory
1 Cyclotron Road
Berkeley, California 94720

October, 1988

This work was supported by the Director, Office of Energy Research, Office of Basic Energy Sciences, Chemical Sciences Division of the U.S. Department of Energy under Contract Number DE-AC03-76SF00098

Preparation and Characterization of Novel Boron Nitride Intercalation Compounds and Ag(III) Fluoro-complexes

Steven G. Mayorga

ABSTRACT

This research exploits the extraordinarily stable anions, SO_3F^- and MF_6^- (M = As, Sb) to stabilize cationic entities such as $(BN)_x^+$, O_2^+, and AgF_2^+ in the preparation of novel materials. The metal pentafluoride in combination with fluorine is a powerfully oxidizing system producing AsF_6^- and SbF_6^- or the polymeric anion $Sb_nF_{5n+1}^-$ which stabilize the cationic species.

When hexagonal boron nitride is exposed to $S_2O_6F_2$ it rapidly forms a deep blue intercalation compound of the composition $(BN)_3SO_3F$. The intercalated boron nitride has been demonstrated to have a room temperature specific conductivity 12 orders of magnitude greater than the parent insulating boron nitride, and exhibits a metallic conductivity dependence upon the temperature. Further treatment of $(BN)_3SO_3F$ with AsF_5 alone or AsF_5/F_2 has resulted in the formation of new intercalation compounds formulated as $(BN)_{>9}AsF_5SO_3F$ and $(BN)_{>4.8}AsF_6$, respectively. A mixture of SbF_5/F_2 will spontaneously oxidize boron nitride producing a boron nitride fluoroantimonate compound, $(BN)_x(SbF_5)_nF$. Attempts to intercalate BN with some very powerfully oxidizing noble metal hexafluorides, MF_6 (M = Os, Ir, Pt), have resulted in the oxidation of BN to BF_3 and N_2 with the corresponding reduction of MF_6 to lower metal fluorides or the metal. In none of the boron nitride intercalation compounds studied have stages higher than the first been observed. These materials appear to be neither thermodynamically nor kinetically stable.

Evidence is given for the reversible dissolution of dioxygenyl salts in thoroughly dried HF. The colorless solution and lack of evolved volatile gas suggest than the oxygen dissolves as the dioxygenyl cation, O_2^+, rather than as the neutral O_2F species. Further evidence is presented for the composition of the purple compound produced from the reaction of Cl_2 with O_2^+ supporting a 1:1 cationic radical species, $(O_2Cl_2)^+$.

Evidence is presented for the existence of the silver (III) fluoro-cation, AgF_2^+. When AsF_5 is placed on AgF_2 in anhydrous HF solution the Ag(II) undergoes a disproportionation to Ag(I) and Ag(III). The Ag(I) of this mixture is oxidized to Ag(III) by exposure to F_2 producing a homogenous deep blue solution of AgF_2^+ shown to be diamagnetic. When the HF is evacuated from the solution containing AgF_2^+ a paramagnetic blue solid is produced, identified to be $AgF^+AsF_6^-$. This Ag(II) compound disproportionates when HF is redistilled back onto the solid producing a mixture of Ag(I) and Ag(III) which can readily be re-oxidized back up to the soluble Ag(III) entity. This redox cycle is reversible with respect to the addition and removal of F_2.

To my parents
for their love, encouragement and constant support
regardless of the path I choose to follow

TABLE OF CONTENTS

LIST OF FIGURES

LIST OF TABLES

CHAPTER I

GENERAL INTRODUCTION

This thesis consists of two main experimental sections. The first part of the thesis (Chapters III and IV) is concerned with the study and characterization of boron nitride intercalation compounds. In Chapter III the stability, structural and electronic properties of boron nitride fluorosulfate, $(BN)_xSO_3F$, are examined. Comparisons are made between this boron nitride compound and its graphite analogue. Chapter IV describes several synthetic strategies that were used to prepare new intercalation compounds of boron nitride. A number of oxidation reactions were explored including the direct interaction of the oxidizing species with boron nitride and displacement reactions, involving the displacement of previously intercalated guest species with another fluoroanion precursor. In Chapter V the reaction of BN with several noble metal hexafluorides is discussed. The second part of the thesis involves two topics in fluorine chemistry. Chapter VI discusses some of the chemistry of dioxygenyl fluorometallate salts, $O_2^+MF_6^-$, and studies which exploitated these powerful oxidizers in attempts to prepare novel fluorometallate species. Of particular interest is the 1:1 adduct formed between Cl_2 and $O_2^+MF_6^-$. The final chapter outlines some recent work that has been done with the silver fluoroarsenate system. In this system the Ag(II) appears to be reversibly oxidized to Ag(III) by molecular fluorine.

CHAPTER II

EXPERIMENTAL APPARATUS AND CHARACTERIZATION

A. Apparatus

In general most of the chemicals used and materials synthesized in this research were extremely moisture sensitive and oxidatively unstable. These materials were manipulated in either a dry argon or nitrogen atmosphere and were stored in stainless-steel, Teflon-FEP, or occasionally thoroughly dried glass or quartz.

1. Vacuum Line

Chemical reactions were carried out primarily on a stainless-steel vacuum line consisting of two main parts: the first of low pressure and the second of high pressure system components. The low pressure system consists of 1/4 " stainless-steel tubing joined together by cross or T-shaped Swagelok connectors with stainless-steel ferrules. The line opened via five ports used for attachment of reaction vessels. Pressure was monitored by a Varian thermocouple gauge (0 - 2000 mtorr) and a Helicoid gauge (0 - 1500 torr). Fluorine and other corrosive materials could be disposed of by initially channelling the effluent through a soda-lime tower, then through a Pyrex cold-trap held at liquid nitrogen temperature. The mechanical pump was connected to the vacuum line through the cold trap. Fluorine could be accessed through the high pressure part of the line which was constructed of Autoclave Engineering valves and tubing. A high pressure gauge (500 psi) was attached to the Autoclave system to monitor fluorine pressure. Quantities of gases could be measured tensimetrically by

utilizing a calibrated section of the low pressure system.

For experiments which required the simultaneous use of a fluoroacid, such as AsF_5, and anhydrous HF, special precautions were taken to avoid direct contact of the liquid with the metal vacuum line. In such instances a separate reaction system was attached to the main vacuum line which consisted of all Teflon-FEP tubing and connectors with Teflon or Kel-F valves.

The main vacuum line required some periodic maintenance such as occasionally cleaning the line and passivating the system. Passivation was generally accomplished by exposing the vacuum line to approximately 1 atmosphere F_2 pressure for several hours. If a fluoroacid or anhydrous HF was to be used in an experiment the line was pre-passivated by exposure to the particular reagent.

2. **Reaction Vessels**

Many different types of reaction vessels were used over the course of this research. Reactors were often constructed individually to meet the requirements of that particular experiment. Generally, reactions were run in either Teflon-FEP or stainless steel reaction vessels, and when conditions permitted, quartz or glass was used. The Teflon vessels (3/8 " or 1/2 " o.d.) were adapted to 1/4" stainless-steel tubing via Swagelok compression fittings to low pressure stainless-steel Whitey valves, or (in the HF/acid work) Kel-F or Teflon valves especially constructed for the purpose. For moderately high pressure (3 - 20 atm) or high temperature (>150°C) reactions small stainless-steel bombs were used that were constructed by boring out 3/8" steel rod. For high pressure reactions requiring greater volume, such as the bulk synthesis of starting materials, Monel cans fitted with removable water-cooled lids were employed. Some reaction vessels were constructed such that the material produced could be

readily transferred to a quartz or Teflon capillary for *in situ* powder X-ray examination.

3. **Dry Box / Glove Bag**

Low volatility materials were routinely handled in an argon atmosphere Dri-lab (Vacuum Atmosphere Co., North Hollywood, CA). The drying trains were regenerated on a regular schedule and the condition of the atmosphere was monitored for moisture by exposing it to an incandescent filament.

Air sensitive, volatile liquids were handled in a glove bag with dry nitrogen used as the circulating gas.

B. **Methods of Characterization**

1. **X-ray powder photography**

General Electric Debye-Scherrer powder cameras (450 mm circumference) were used for routine structural analysis of powdered samples. Nickel filtered Cu Kα radiation was used for all photographs. Quartz or glass capillaries (3,5 or 7mm ; Charles Supper Co.) were used for most samples. When conditions required, Teflon capillaries were employed. For low temperature X-ray studies a stream of cold nitrogen was run over the sample along with a stream of warm nitrogen around the periphery to minimize water condensation. Capillaries were routinely loaded in the dry box and temporarily sealed with Kel-F grease until they could be sealed with a micro-torch outside of the box.

2. **Infra-red Spectroscopy**

Infrared spectra were recorded on a Nicolet 5DX Fourier Transform Spectrophotometer and on a Perkin-Elmer 591 Spectrophotometer. Gaseous spectra were run in a 10 cm path length Monel cell equipped with silver chloride

windows (cell vol. ≈ 130 cc). The silver chloride windows were secured to the Monel cell by means of Teflon o-rings which provided an air-tight seal. The cells were passivated when necessary prior to use. Solid samples were run either in KBr pellets, or in a Teflon cell equipped with AgCl windows.

3. **Raman Spectroscopy**

Raman Spectra were recorded on a Jobin-Yvon HG2S spectrometer using a krypton (647.1 nm) laser as the exciting source. Samples were run in 1.0 or 1.5 mm quartz capillaries.

4. **Four-probe Conductivity**

Temperature dependent electrical conductivity measurements were made using the four-probe technique on pressed pellets of powder samples. The apparatus consisted of a Pyrex flask fitted with a ground glass insert through which 4 platinum wires and a Cu-constantine thermocouple wire were threaded. The platinum wires were attached in a parallel arrangement approximately 1.0 mm apart to a Teflon plate onto which the sample could be loaded and secured in the Dri-lab. The flask was equipped with a valve through which the sample could be evacuated and repressurized with a helium atmosphere. By circulating a stream of cold N_2 over the flask the temperature could be precisely regulated for temperature dependent studies. A power supply was used to apply a potential across the outer leads while the change in current was measured by a hand-held voltmeter across the inner leads.

5. **Magnetic Susceptibility**

a. **Faraday Balance**

Room temperature magnetic measurements were performed on a Johnson

Matthey Magnetic Susceptibility Faraday Balance. Powdered samples were run in run in specially constructed Pyrex tubes. Susceptibility measurements for samples in HF solution were run in Teflon-FEP tubes. For weakly paramagnetic or diamagnetic samples the measured susceptibility was corrected for the diamagnetic contribution[1,2]. Further details concerning the use of the instrument are give in Chapter VII.

6. **Elemental Analysis**

Standard elemental analysis was done by the Analytical Laboratory, Department of Chemistry, UC Berkeley. Analysis for chlorine in the O_2^+/Cl_2 complexes was done in this laboratory by first reducing the chlorine in the sample to chloride by reaction with NO and water, then titrating with standard $AgNO_3$ to a pink endpoint indicating the formation of the complex between excess Ag^+ ion and the chlorofluoroscein indicator. Analysis for evolved molecular fluorine was done by evacuation through a Teflon-FEP U-trap containing KI. The iodine produced was titrated with standard thiosulfate solution using a starch indicator. A detailed description of the analyses is given by Vogel[3].

CHAPTER III

BORON NITRIDE FLUOROSULFATE

A. Introduction / Background

Hexagonal boron nitride is isoelectronic with graphite and has a similar hexagonal layered structure. Each layer is composed of a planar network of B_3N_3 hexagons (see fig. 3.1). The largest difference between the graphite and layer boron nitride structures lies in the relative stacking of the planes. In boron nitride the hexagons of adjacent sheets are eclipsed with the boron atoms always overlying nitrogen atoms of the adjacent sheets whereas in graphite the hexagons of adjacent sheets are staggered in an AB sequence with half of the carbon atoms eclipsing adjacent sheet neighbors. The unit cell parameters of boron nitride are quite similar to those of graphite, with Z = 2 for both materials. Despite these structural similarities these materials exhibit strikingly different electrical properties. Due to the heteronuclear character of boron nitride the electrons are not as extensively delocalized as in the graphitic system. Boron nitride is a white insulating material with a band gap[4] of 4 eV whereas graphite is a dark gray semi-metal with a small band overlap[5] of approximately 0.04 eV (see fig. 3.2).

These similarities between the graphite and boron nitride systems suggest a comparative study of the intercalation chemistry they undergo. There have been several reports of synthesis of boron nitride compounds. Croft had reported[6] a small weight increase resulting from the interaction of BN powder with $FeCl_3$, $AlCl_3$, or NH_3. He also observed that some of these materials exfoliated upon heating. However, Rudorff and Stumpp[7] in later experiments could not

reproduce Croft's observations, suggesting that his "glossy black" BN starting material may have been impure. Freeman and Larkindale[8,9] reported a pink product from the interaction of BN with $FeCl_3$ accompanied by a small expansion of the interlayer spacing. However, Ohashi and Shinjo[10] studied this system extensively and concluded that this pink material was due to the surface hydrolysis product FeOCl. FeOCl is itself is a layered structure material with the PbFCl structure[11]. There also have been several reports of reductive intercalation of BN[12] using alkali metals (K, Cs). These were based on a few percent weight increase, but once again reproducibility has not been established. Perhaps the best substantiated of these claims was the reported synthesis of boron nitride fluorosulfate first prepared in this laboratory[13,14]. This system was extensively reinvestigated in the present research.

The process of intercalation can be divided into several thermodynamic steps. In fig. 3.3 a general Born-Haber cycle for the oxidative intercalation of boron nitride is shown. There are two endothermic and two exothermic processes. Energy must be spent to expand the sheets to the appropriate separation distance to accommodate the intercalant guest species. The sheets are held together by a weak van der Waals attraction due to the overlap of the π band of the B-N system, and by an electrostatic attraction caused by the alternate arrangement of the B and N atoms of adjacent sheets. Another endothermic step involves the removal of an electron from the boron nitride sheets. These two processes must be offset by the electron affinity of the oxidizing agent and the lattice energy of the resulting salt if the overall process is to be exothermic ($\Delta H_{rxn}° < 0$). ΔS_{rxn} is negative due to the greater order of the product relative to the reactants, hence an appreciable exothermicity is required to offset the unfavorable $T\Delta S$ term in ΔG.

The oxidative intercalation of boron nitride is especially precarious due to its

limited stability in the presence of anhydrous hydrogen fluoride or fluorine. In anhydrous hydrogen fluoride boron nitride is quantitatively converted to ammonium tetrafluoroborate[15]:

3.1) $BN + 4HF \rightarrow NH_4^+BF_4^-$

and in the presence of fluorine the following reaction occurs slowly at room temperature:

3.2) $2BN + 3F_2 \rightarrow 2BF_3 + N_2$

ESCA studies[16] have shown the B of boron nitride to be slightly positive (+0.3 e) and the N to be slightly negative (-0.3 e). The positive boron centers may be especially vulnerable to attack by HF_2^- or F^-. A good candidate for oxidative intercalation of boron nitride ought to be a material which is a strong electron oxidizer yet a poor fluorinating agent, and the precursor of an anion of high kinetic stability, such is the case with peroxydisulfuryl difluoride, $S_2O_6F_2$, which is the source of SO_3F radical: $S_2O_6F_2 \rightleftarrows 2SO_3F\cdot$ and the precursor for SO_3F^-.

As previously mentioned graphite is a semimetal while boron nitride is an insulator. A simple band diagram model comparing the two is shown in fig. 3.2. The room temperature specific electrical conductivity of graphite[17] varies from about 100 - 20,000 ohm^{-1} cm^{-1} (depending upon its purity and crystallinity). By contrast, boron nitride is an excellent electrical insulator[18] with a reported conductivity of 10^{-12} $ohms^{-1}$ cm^{-1}. The insulating nature of boron nitride is in harmony with the large band gap separating the valence and conduction bands.

Oxidized graphite intercalation compounds were first shown[19,20] by Ubbelohde and coworkers more than forty years ago to be excellent electrical conductors. They demonstrated that the conductivity of the graphite compound was approximately one order of magnitude more conductive than the parent graphite. This enhanced conductivity, which in some cases exceeds that of aluminum metal, is due to the increased number of electron hole carriers resulting from

creation of holes in the valence band. Similarly, one might anticipate oxidized BN salts to exhibit greatly enhanced electrical conductivity for the same reason. The preliminary work of Biagioni in these laboratories[14] indicated that this was so, but Hooley[21] had failed to confirm high electrical conductivity in the $(BN)_xSO_3F$ samples that he studied. Accordingly, the first work in the BN intercalation study was to carry out a dependable conductivity measurement on a BN fluorosulfate of known composition.

Experimental

1. Starting materials

Microcrystalline boron nitride (325 mesh) supplied by Ventron (Beverly, Mass.) was used for most of the work described. In a few experiments for the purpose of making comparative conductivity studies, one cm^2 plates of highly oriented boron nitride, HOBN, were used (Union Carbide). In all instances boron nitride was pretreated by thoroughly flaming with a gas-oxygen torch in a quartz tube under vacuum. Samples of boron nitride thus prepared were stored in sealed quartz tubes in the Dri-lab until needed.

Peroxydisulfuryl difluoride, $S_2O_6F_2$, was typically prepared in 2 or 3 ml quantities according to the following two main reaction schemes[22,23]:

3.3) $XeF_2 + 2HSO_3F \rightarrow Xe(SO_3F)_2 + 2HF$

3.4) $XeF_2 + 2\ SO_3 \rightarrow Xe(SO_3F)_2$

The resulting divalent xenon compound was then gently warmed to facilitate decomposition:

$$\xrightarrow{40°C}$$

3.5) $Xe(SO_3F)_2 \rightarrow S_2O_6F_2 + Xe$

In addition, to assess its suitability for large scale synthesis, $S_2O_6F_2$ was prepared according to a procedure given by Šmalc[24]:

3.6) $2HSO_3F + 2O_2^+AsF_6^- \rightarrow S_2O_6F_2 + 2HF + 2AsF_5 + 2O_2$

In all preparations the colorless liquid product was distilled and was then characterized by its vapor pressure and infra-red spectrum[25]. The distilled product was stored over XeF_2 in Pyrex tubes fitted with stainless steel valves.

The XeF_2 was prepared by exposing a thoroughly dried 5-liter Pyrex bulb containing a 1:1 gaseous mixture of Xe/F_2 to sunlight for two days[26]. Unreacted F_2 and Xe were removed and the remaining solid XeF_2 was sublimed in a

dynamic vacuum into a Kel-F trap where it was placed in the Dri-lab for storage.

$NO^+SO_3F^-$ was prepared by exposing $S_2O_6F_2$ to an excess of NO at room temperature in a quartz vessel:

3.7) $NO + 1/2\ S_2O_6F_2 \rightarrow NO^+SO_3F^-$

The residual volatile gas was removed by evacuation and the remaining colorless powder was characterized by its X-ray powder diffraction pattern.

Sulfur trioxide, SO_3, and fluorosulfonic acid, HSO_3F were supplied by Allied Chemical Co. (Morristown, N.J.). The SO_3 was stored in a Pyrex container fitted with Teflon-FEP valves to which BF_3 was added to inhibit polymerization. The HSO_3F was distilled and stored in a Pyrex vial prior to use.

2. Reaction of BN with $S_2O_6F_2$

$(BN)_xSO_3F$ was prepared by the reaction of either liquid or gaseous $S_2O_6F_2$ with powdered boron nitride. Typically 50 - 200 mg quantities of BN were loaded into a pre-weighed flamed-out Pyrex or quartz tube in the dry lab, then fitted with a Whitey valve. Excess liquid $S_2O_6F_2$ was condensed onto the BN powder at -78°C (CO_2/acetone bath) such that the BN was completely immersed in the liquid. The reactor was warmed to room temperature and the reaction allowed to proceed. Within 15 minutes the BN became light grey, metal grey, then finally navy blue in color. The reaction was usually complete within about half an hour. Unreacted $S_2O_6F_2$ was removed by evacuation and the sample was further evacuated for approximately 5 - 10 minutes yielding a blue friable solid.

Several attempts were made to obtain an improved X-ray powder pattern of $(BN)_xSO_3F$ by performing *in situ* capillary intercalation reactions, thus avoiding handling the material in the Dri-lab. In these experiments BN was placed in a 1/4 " (o.d.) Pyrex tube, fitted to a Whitey valve on one side and drawn down to

a 0.8 mm capillary on the other.

On a number of occasions $(BN)_xSO_3F$ was prepared by the room temperature reaction with $S_2O_6F_2$ vapor. In these experiments the boron nitride was placed at the base of a Pyrex tube equipped with a small side-arm. Excess $S_2O_6F_2$ was condensed into the side-arm and allowed to warm to ambient temperature (P_{vap} = 130 torr). Within a period of 3 - 4 hours the reaction was complete yielding the navy blue salt.

Highly oriented BN (HOBN) was reacted with liquid $S_2O_6F_2$ on several occasions with the intent of obtaining basal-plane conductivity measurements. In all such reactions intercalation proceeded considerably more slowly and to a lesser extent than in the analogous preparations involving powdered BN. Several hours were needed before the reaction was complete.

3. Attempts to prepare higher stage $(BN)_xSO_3F$

Attempts were made to prepare higher stage salts by three methods: (1) limited exposure of BN to $S_2O_6F_2$, and (2) subjecting a freshly prepared sample of $(BN)_3SO_3F$ to a dynamic vacuum and (3) mechanically mixing $(BN)_3SO_3F$ with the appropriate amount of BN to give a second-stage salt. Structural changes were monitored by X-ray analysis.

In the first investigation carefully measured amounts of $S_2O_6F_2$ were condensed onto the BN according to the stoichiometry $(BN)_{6-8}SO_3F$. The samples were then agitated for several hours by either a fan or a mechanical vibrator. Powder photographs of the resulting products consistently indicated a two phase mixture of BN and $(BN)_3SO_3F$. In the second method mentioned above, the first-stage salt had been observed to completely decompose when subjected to a dynamic vacuum for two hours (see p. 22). Investigating the possibility that the process of de-intercalation involves higher stage

intermediates, a newly prepared sample of $(BN)_3SO_3F$ was exposed to dynamic evacuation for one hour, removing powdered samples for X-ray analysis at time intervals of 20 minutes. The photographs showed only a mixture of BN and $(BN)_3SO_3F$ with no indication of a higher stage salt. After twenty minutes of evacuation the powder photograph showed a dominant $(BN)_3SO_3F$ pattern and a weaker BN pattern, while after 60 minutes of evacuation the BN pattern was dominant. The third method involved mechanically agitating a physical mixture of BN and $(BN)_3SO_3F$ for two days. Again, this method proved unsuccessful, yielding a somewhat less crystalline $(BN)_3SO_3F$ and BN.

4. **Reaction of $(BN)_xSO_3F$ with $S_2O_6F_2$ and HSO_3F.**

A number of attempts were made unsuccessfully to incorporate HSO_3F into $(BN)_xSO_3F$. BN and excess HSO_3F were placed in a Teflon tube and fitted with a Whitey valve in a glove bag with no noticeable reaction. Subsequently, excess $S_2O_6F_2$ was condensed on the mixture at -78°C and allowed to warm to ambient temperature. The reactor was agitated by means of an electric fan. Within half an hour a dark blue solid wet with HSO_3F was obtained. Attempts to remove the HSO_3F by dynamic evacuation resulted in the loss of color intensity of the blue solid which had evidently decomposed.

Similar experiments were run in which known amounts of HSO_3F were added to BN samples then subsequently treated with $S_2O_6F_2$ in an attempt to produce intercalation compounds of the general formula $(BN)_x^{y+}(SO_3F^-)_y(HSO_3F)_{1-y}$. Three such experiments were attempted, varying the fluorosulfonic acid content (y = 1/3, 1/2, 2/3). Such experiments didn't require evacuation of HSO_3F from the final product.

5. **Product Analysis**

Debye-Scherrer powder diffraction was the principle method used for structural analysis of the intercalation compounds produced. Chemical composition and thermal and vacuum stability of the BN salts were monitored by gravimetry, tensimetry and infra-red analysis. The specific electronic conductivity was measured as a function of temperature ($100K < T < 293K$) by the four-probe method.

C. Observations and Results

1. Composition

BN with $S_2O_6F_2$ (*l*) The composition of the salt resulting from the interaction of liquid $S_2O_6F_2$ with BN was determined by exposing the BN to an excess of the oxidizing liquid, evacuating the $S_2O_6F_2$, venting to 0 torr by a brief 5-10 minute evacuation, then measuring the weight increase. The composition was consistently evaluated (see table 3.2a) by a number of such runs to be $(BN)_{3.0}SO_3F$, corresponding to a densely packed first-stage salt. Unlike its graphite analogue[14], C_xSO_3F ($x \approx 7$), this salt is not vacuum stable but decomposes rather rapidly upon dynamic evacuation. The specific decomposition products are discussed in detail later in this chapter.

BN with $S_2O_6F_2$ (g). Gaseous $S_2O_6F_2$ interacted with BN to give eventually the same compound as obtained with liquid $S_2O_6F_2$. Generally, a four hour exposure of BN to $S_2O_6F_2$ vapor was sufficient to give a gravimetry corresponding to $(BN)_3SO_3F$ (table 3.2a). A two hour reaction time yielded a less intensely colored blue material with the composition "$(BN)_{4\text{-}5}SO_3F$" which was later shown to be simply a mixture of BN and $(BN)_3SO_3F$.

BN with $S_2O_6F_2$ and HSO_3F. As previously mentioned the nonvolatility of HSO_3F and the lack of stability of $(BN)_3SO_3F$ towards dynamic evacuation suggested synthesizing an acid-containing boron nitride fluorosulfate by initially adding a predetermined amount of HSO_3F to BN then treating with excess $S_2O_6F_2$ with the intent of producing BN intercalation compounds of the general formula $(BN)_x^{y+}(SO_3F^-)_y(HSO_3F)_{1-y}$. Such an experimental design circumvents removal of excess HSO_3F by dynamic evacuation, and hence avoids possible

decomposition of the BN salt. Three such experiments were attempted, varying the fluorosulfonic acid content (y = 1/3, 1/2, 2/3). In these experiments there was no evidence of reaction after initially placing the HSO_3F on BN. However, upon condensing on excess $S_2O_6F_2$ the mixture assumed a light blue color. The samples were briefly evacuated to pull off the excess $S_2O_6F_2$ leaving behind a pasty blue material. The X-ray powder pattern showed predominantly $(BN)_3SO_3F$ with a trace of BN and there was no increase in the c-spacing that would likely accompany HSO_3F incorporation. The gravimetry of the products was accounted for in terms of formation of $(BN)_3SO_3F$ with residual HSO_3F. No further attempts were made to incorporate the acid into boron nitride fluorosulfate.

2. Staging

The $(BN)_3SO_3F$ prepared by the interaction of powdered BN with excess $S_2O_6F_2$ was invariably first-stage with a c-axis repeat distance of 8.06(2) Å. The failure to observe higher stage boron nitride fluorosulfate stands in sharp contrast to the ease with which higher stage graphite fluorosulfates are formed. Second-stage C_xSO_3F can readily be prepared by exposing graphite to a carefully controlled pressure of $S_2O_6F_2$. This second-stage compound thus prepared is a vacuum-stable dark blue material.

The instability of higher stage BN compounds may be largely due to the heteronuclear character of BN. As mentioned earlier, ESCA measurements have demonstrated that the boron atoms carry a partial positive charge and the nitrogen atoms a partial negative charge. This polarity of the sheets must result in a larger energy of sheet separation than in graphite, hence at first glance the BN situation appears to be conducive to higher stage salts. However, as pointed out by Daumas and Hérold[27] in the case of graphite, staging is integrally tied to domain formation and a second-stage salt, therefore, has the appearance

shown below:

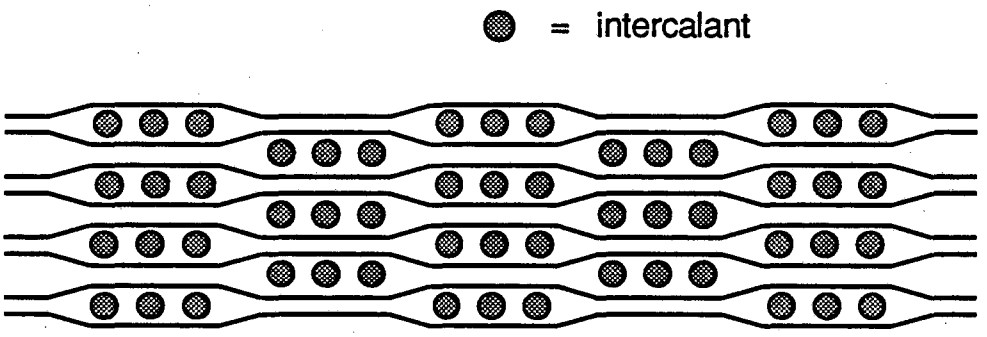

Clearly staging demands extraordinary sheet flexibility and it may be the diminished flexibility of the BN sheets as a consequence of the very different sizes of the B and N p_z functions that lies at the basis of this apparent failure of BN to form higher-stage BN salts.

Another and perhaps more important reason for the non-existence of higher stage $(BN)_ySO_3F$ salts has to do with the disposition of the positive charge in the BN sheets. As electrons are removed from the sheets the boron atoms will, on the average, become even more positive and these atoms in particular will tend to be aligned in closest approach to the anions placed between the sheets. This will pull the enclosing BN sheets into alignment as illustrated below.

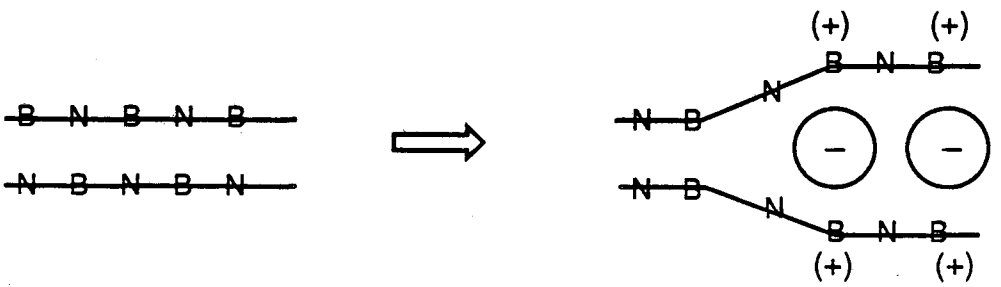

unintercalated BN intercalated BN

Thus, in the unintercalated regions the facing atoms are now of like kind and charge. The realignment therefore helps, by the mutual repulsion of the facing B or N atoms, to separate the sheets and support the further intercalation.

3. Structure

The established composition for the pure first-stage boron nitride fluorosulfate compound is $(BN)_{3.0}^{+}SO_3F^{-}$ (table 3.2a). One can readily calculate the theoretical composition for a two-dimensional closed-packed arrangement of tetrahedral fluorosulfate ions between enclosing BN layers by estimating the molecular volume required for the SO_3F^{-} ion and knowing the volume between the intercalated BN sheets available for guest species. The volume of the SO_3F^{-} ion can be estimated by considering the volume of $K^{+}SO_3F^{-}$. $K^{+}SO_3F^{-}$ crystallizes in the orthorhombic space group Pnma with a unit cell volume of 370.0 Å^3, and Z = 4[28]. Therefore, $V_{(formula\ unit)}$ = 92.5 Å^3. The volume of K^{+} should be approximately 17 Å^3 as calculated from its estimated ionic radius of 1.6 Å[29]. Hence the volume of SO_3F^{-} should be 92.5 $Å_3$ less 17 Å^3, or approximately 75 Å^3. Recalling that first-stage boron nitride fluorosulfate has an interlayer spacing of 8.06(2) Å and allowing a van der Waals layer thickness of 3.33 Å for the π clouds of the BN sheets, there remains a 4.73 Å height available for packing of the SO_3F^{-} ions. Since there is one BN per pseudo-unit cell in the first-stage BN salt the volume available for anions per BN can be estimated:

$$V_{(anions)}/\ BN = a^2h(\sin 60°) = (2.464\ Å)^2(4.73\ Å)(\sin 60°)$$
$$= 24.9\ Å^3$$

since the volume of SO_3F^{-} is ≈ 75.3 Å^3 the composition of first-stage boron nitride fluorosulfate containing closed-packed tetrahedra is estimated to be $(BN)_{3.02}SO_3F$, which agrees well with the experimentally observed composition.

The orientation of the SO_3F^{-} ion within the BN sheets has not been directly experimentally determined. Aubke and his coworkers[30] have done some recent work with first-stage graphite fluorosulfate, C_7SO_3F, in which he has examined

the orientation of SO_3F^- within the graphite host gallery through a series of ^{19}F n.m.r. studies. By performing an angular dependence study on HOPG fluorosulfate it was concluded that the majority of the intercalated SO_3F^- ions are oriented with their molecular C_3 symmetry axis parallel to the c-axis of the HOPG salt.

Insight into the orientation of the fluorosulfate ion within the BN galleries can be gained by considering the interlayer spacing of $(BN)_3SO_3F$. Two reasonable possibilities exist for the orientation of SO_3F^- which would permit efficient packing and be allowed by the observed c-spacing. The two orientations, A and B, with their respective interlayer spacings are shown in fig. 3.4. Possibility A has the SO_3F^- ion oriented with a pseudo two-fold axis parallel to the c-axis of BN, and the second possibility has a three-fold axis of SO_3F^- aligned with the c-axis of BN.

The calculated distances for the intersheet spacing corresponding to these two anionic orientations are 7.80 Å and 8.06 Å, respectively. To arrive at these distances SO_3F^- is treated as an ideal tetrahedron with a S-ligand bond distance of 1.46 Å, which is the weighted average of the S-O and S-F bond distances in the potassium and ammonium salts of SO_3F^- [28,31]. The weighted Pauling's van der Waals radius for the ligands is 1.39 Å, and the thickness of the BN van der Waals layer is taken to be 3.33 Å.

Anionic orientation B is preferred for several reasons over orientation A. Arranging the SO_3F^- ions with a three-fold axis parallel to the c-axis permits the anions to form a closed-packed two-dimensional layer. Consequently, each SO_3F^- ion is surrounded by three inverted SO_3F^- ions *ad infinitum* comprising the anionic sheet layer illustrated in fig. 3.4. As demonstrated, such a closed-packed network is required to account for the observed composition. Orientation A does not allow a two-dimensional network of completely closed-packed

tetrahedra, and, therefore, is inconsistent with the composition $(BN)_3SO_3F$. Orientation B also has a calculated interlayer spacing (8.06 Å) which agrees with the observed c-spacing [8.06(2) Å].

The c-spacing of first-stage boron nitride fluorosulfate is about 0.45 Å greater than the c-spacing of the analogous graphite salt (8.06 Å versus 7.6 Å), despite the similarity of the c_o parameters for boron nitride and graphite. This discrepancy can be accounted for by assuming that the SO_3F^- anions are "nestled" in the graphite salt, but "un-nestled" in the BN salt.

Bartlett and Okino[32] developed a nestling model which explains the low observed intercarbon spacing, I_c, spacing of 7.6 Å for first-stage vacuum-stable $C_{14}AsF_6$. In order to accommodate the AsF_6^- octahedral anions within the graphite host lattice the octahedra must be aligned such that a three-fold axis is parallel to the c-axis of graphite with the F ligands nestling into the center of the graphite hexagons of adjacent sheets. Such a geometrical arrangement requires that any two enclosing graphite sheets are positioned in an AB staggered fashion.

Okino observed that addition of AsF_5 to a vacuum-stable $C_{14}AsF_6$ salt produces a structurally different material with an expanded interlayer spacing of 8.0 Å. A structural model has been developed to account for this observation in which the AsF_x species are un-nestled within the host galleries, and accordingly, the carbon atoms of one sheet are eclipsed with those of adjacent sheets.

The nestled structure requires that the 6 F ligands must be centered in the cavities of the C_6 rings and approximately 0.2 Å below the top of the π cloud of the host lattice. This arrangement is possible only because of the geometrical coincidence that the F-F ligand distance of an MF_6 octahedron is compatible with the distance separating the centers of neighboring carbon hexagons.

The SO_3F^- anion is a pseudo-tetrahedron with an average S-ligand bond

distance of 1.46 Å. For an ideal tetrahedron with a bond distance of 1.46 Å the ligand-ligand distance would be $2(\sqrt{2}/\sqrt{3})(1.46\ Å) = 2.38\ Å$. This distance is close to the lattice constant a_o of graphite (2.50 Å), which, by definition, is the distance separating the centers of neighboring hexagons. If the SO_3F^- anions are oriented with a three-fold axis parallel to the c-axis of graphite some degree of nestling should be allowed. If each of the ligands of the SO_3F^- anions nestled $\approx$ 0.2 Å beyond the top of the π cloud of the graphite lattice, as do the F ligands of the vacuum stable $C_{14}AsF_6$, then a 0.4 Å I_c contraction would be anticipated. Hence the first-stage boron nitride fluorosulfate interlayer spacing [8.06(2) Å] is consistent with an un-nestled arrangement of closed-packed SO_3F^- tetrahedra and the corresponding graphite salt possessing a gallery height of 7.60 Å is consistent with a nestled tetrahedral arrangement. An illustration of this model is given in fig. 3.5.

The powder patterns of $(BN)_3SO_3F$ obtained in this research indicate that there is some sheet-to-sheet registry between the BN layers. The powder data consist of (*h*00), (00*l*), and some general (*hkl*) reflections. In powder patterns of some of the more crystalline samples the (111) and (112) reflections are observed (table 3.1).

3. Stability

Vacuum. $(BN)_3SO_3F$ does not appear to be vacuum stable but will de-intercalate rapidly upon evacuation to a colorless material. When subjected to a dynamic vacuum a freshly prepared sample of $(BN)_3SO_3F$ loses $S_2O_5F_2$ (g) in concert with $NO^+SO_3F^-$ formation. The decomposition is believed to proceed according to the following equation:

3.8) $$6(BN)_3SO_3F(s) \rightarrow 17\ BN(s) + 2\ 1/2\ S_2O_5F_2(g) + NO^+SO_3F^-(s) + 1/2\ B_2O_3(s)$$

Gravimetry (see table 3.2b) consistently indicated that after two hours of evacuation the product weighed approximately 55% of the starting material (see fig 3.6). This is in excellent agreement with that predicted by the stoichiometry of the reaction shown above, recognizing that $S_2O_5F_2$ would be lost as a volatile product. The X-ray powder pattern of BN always appeared strongly in the decomposition product, it being absent in that of the freshly prepared $(BN)_3SO_3F$.

During a two hour evacuation period the volatile decomposition products were collected in a stainless steel U-trap at 77 K. The trap was allowed to warm to room temperature and the contents were expanded into an infra-red cell and shown to be $S_2O_5F_2$ with no indication of $S_2O_6F_2$, other sulfur oxyfluorides or BF_3. BN and $NO^+SO_3F^-$ were seen by X-ray diffraction. In order to detect $NO^+SO_3F^-$ it was necessary to re-expose the solid decomposition products to $S_2O_6F_2$ and evacuate once again. After 3 or 4 such cycles enough $NOSO_3F$ had accumulated to be detected by X-ray analysis. B_2O_3 is believed to be a product, but may not be detectable by diffraction due to its glassy nature.

The decomposition reaction shown above (eq. 3.8) is not reversible at ambient temperature. To check the reversibility a freshly prepared sample of $(BN)_3SO_3F$ was evacuated for 5 hours yielding a colorless solid. Approximately 10 atmospheres of $S_2O_5F_2$ was placed over the colorless solid for $\approx$ 4 hours. No coloring of the solid was observed and the powder pattern indicated no chemical reaction with $S_2O_5F_2$.

Thermal. $(BN)_3SO_3F$ doesn't appear to be thermally stable as indicated by its reported detonation upon warming to 40°C[13]. In the present research a detonation was not observed upon warming to 100°C, however, the system rapidly evolved $S_2O_5F_2$ when heated in a static vacuum. Heating must facilitate the decomposition process shown above in eq. 3.8.

4. Electrical Conductivity

Contactless technique. Most of the previous conductivity measurements of graphite intercalation compounds were done by a contactless inductive method[33] which measures the basal-plane conductivity. This technique is particularly attractive because of the relative ease with which accurate, in situ measurements of layered materials can be obtained; however, highly conductive HOPG or HOBN samples are required and this technique does not readily lend itself to temperature dependant studies. The intercalation compounds prepared from HOBN samples in the present research unfortunately were not conductive enough to give meaningful results from this technique. However, the contactless technique was employed to determine the conductivity of graphite fluorosulfate samples, C_xSO_3F, prepared from HOPG for the purpose of a comparative study with the BN system.

Four-Probe technique. The specific conductivity of $(BN)_3SO_3F$ was determined by using the four-probe technique described earlier. Powdered polycrystalline samples were prepared for conductivity measurements by pressing into pellets in the Dri-lab using an IR hand-cranked pellet press. The pellets were cut into thin rectangular pieces with a razor blade of the approximate dimensions: thickness = 0.5 mm, length = 8 mm, and width = 3 mm. The rectangular pellets were placed across the platinum leads and secured with a Teflon holder (see fig. 3.7). A current was applied across the outer leads and the voltage was measured across the inner leads. The air-tight apparatus was removed from the Dri-lab and the argon atmosphere was evacuated and repressurized with helium for the purpose of having an efficient medium for thermal conduction. The sample temperature could be varied from 100(5) K to 293 K for temperature dependant

studies by carefully regulating the flow rate of a stream of cold nitrogen over the apparatus contained in a Dewer. An illustration of the four-probe device is given in fig. 3.7.

The specific conductivity (ohm^{-1} cm^{-1}) at a given temperature is given by the following equation:

3.9) $\sigma = (l/A)(1/R)$

where l (cm) is the length between the two inner platinum leads, A (cm^2) is the cross-sectional area of the sample, and R (ohms) is the resistance. The resistance is simply the ratio of the applied voltage to the current flowing between the central leads. A series of readings were routinely taken varying the potential to check for current-voltage linearity, and the polarity was reversed to confirm the low ohmicity of the contacts. Measurements for any given sample were reproducible to within ± 10%.

<u>$(BN)_xSO_3F$.</u> The room temperature specific conductivity (four-probe) of a pressed pellet of freshly prepared $(BN)_3SO_3F$ varied from 1-4 ohm^{-1} cm^{-1}. This represents an increase of more than 12 orders of magnitude over the parent BN. The conductivity showed a slight metallic temperature dependence increasing by 20-25% as the temperature was dropped from 293 to 100 K (fig. 3.8). It was also observed that incomplete intercalation yielded considerably lower conductivity measurements. On one occasion a sample with a gravimetry corresponding to $(BN)_{42}SO_3F$ gave a conductivity value of 0.03 $ohm^{-1}cm^{-1}$. This reduced value can be accounted for by the presence of small insulating pockets of BN present in the sample.

<u>C_xSO_3F.</u> Samples of first-stage graphite fluorosulfate were prepared in this research for the purpose of conducting a comparative study between BN and

graphite salts. Thoroughly flamed out samples of HOPG and SP1 graphite were exposed to excess $S_2O_6F_2$ for several hours after which the unreacted $S_2O_6F_2$ was removed by evacuation. With SP1 graphite a vacuum stable dark blue material was achieved after two hours of dynamic evacuation whose gravimetry corresponding to $C_{7.5}SO_3F$. This sample yielded a four-probe room temperature specific conductivity value of 1.5×10^3 $ohm^{-1}cm^{-1}$, representing a 2.5-fold increase over the value of 610(40) $ohm^{-1}cm^{-1}$ determined in this laboratory[34] for the conductivity of SP1 graphite.

The intercalation of $S_2O_6F_2$ into HOPG was not quite as facile as in the case of SP1 graphite. This discrepancy can be attributed to the large particle size of HOPG relative to SP1 graphite. After 3 hours of reaction with excess liquid $S_2O_6F_2$, a composition of $C_{10}SO_3F$ was obtained. Longer reaction times (4,6 hrs) failed to yield more fluorosulfate-rich graphite salts. The "$C_{10}SO_3F$" presumably corresponds to a compound which is primarily a first-stage salt with second-stage domains. Upon heating the $C_{10}SO_3F$ sample with $S_2O_6F_2(l)$ to 50°C for 1 hour, then evacuating to constant weight a composition of $C_{8.3}SO_3F$ was obtained. This chip of HOPG salt was placed into a flattened quartz tube for contactless conductivity measurement. The room temperature specific conductivity was determined in this manner to be 1.1×10^5 $ohm^{-1}cm^{-1}$. A previous set of measurements done in this research yielded a conductivity value of 2.2×10^4 $ohm^{-1}cm^{-1}$ for HOPG; therefore, the salt is 5 times more conductive than the parent HOPG.

A crude conductivity-temperature dependent study of the HOPG chip which had a composition of $C_{8.3}SO_3F$ was carried out. The investigation was done by submersing the flattened quartz tube into various temperature baths (0°, -23°, -78°, and -196°C) then immediately placing the tube into the field of the magnet for the contactless measurement. The specific conductivity at -196°C was

3.1×10^5 ohm^{-1} cm^{-1}, representing a 3-fold increase over the room temperature value.

The boron nitride fluorosulfate, like the graphite fluorosulfate, showed a metallic conductivity dependence upon the temperature. The higher observed conductivity of the HOPG and its fluorosulfate salt compared to SP1 graphite and its fluorosulfate salt may be due to the different conductivity measurement techniques as well as the physical nature of the graphites. The conductivity of HOPG and its salt were measured by the contactless technique, which measures the basal-plane conductivity, whereas, the four-probe method, used for the SP1 material, is a bulk measurement which must contain a component of the c-axis conductivity which is considerably lower than the basal-plane conductivity.

D. Discussion

1. Energy Considerations

The oxidative intercalation of BN, as mentioned earlier, apparently requires a reagent which is both a strong oxidizing agent yet a poor fluorinating agent. $S_2O_6F_2$ is a weak fluorinating agent, yet the oxidizing strength of the $SO_3F\cdot$ (with which it is in equilibrium[25]) is not well described since no quantitative study has been done to evaluate its electron affinity. The dimeric peroxide species is in equilibrium with the monomeric radical:

3.10) $S_2O_6F_6 \rightleftarrows 2SO_3F\cdot$

The $SO_3F\cdot$ is a one electron oxidizer. The half reaction is:

3.11) $SO_3F\cdot + e^- \rightarrow SO_3F^-$

The great oxidizing strength of the $SO_3F\cdot$ is nicely illustrated by its ability to spontaneously intercalate graphite and BN to produce first-stage salts. As demonstrated in earlier work by Mallouk and Bartlett[35] there appears to be, for first-stage graphite salts, a free energy threshold for the half-cell reaction of the intercalating species of approximately 120 kcal $mole^{-1}$ associated with the spontaneous intercalation of graphite. Based on this observation the fluorosulfate radical must have a minimum electron affinity of 120 kcal $mole^{-1}$.

An independent assessment of the electron affinity of $SO_3F\cdot$ can be made by noting that $NO^+SO_3F^-$ exists while $O_2^+SO_3F^-$ does not. The overall reactions involved are:

3.12) $NO(g) + SO_3F\cdot(l) \rightarrow NO^+SO_3F^-(s)$

3.13) $O_2(g) + SO_3F\cdot(l) \neq O_2^+SO_3F^-(s)$

The electron affinity of the fluorosulfate radical is large enough to stabilize NO^+, but cannot effectively stabilize O_2^+. Therefore, upper and lower limits of the

electron affinity of $SO_3F\cdot$ can be assigned by an evaluation of the Born-Haber cycle for the above reactions. For spontaneous reactions $\Delta G°_{rxn} < 0$ which requires $\Delta H°_{rxn} < +T\Delta S°_{rxn}$. The reaction enthalpy is the sum of the ionization energy (I) the electron affinity (E) and the lattice energy (U). Therefore, solving for the electron affinity we have:

3.14) $E = T\Delta S°_{rxn} - I - U$

The entropy of $O_2(g)$ and NO(g) are given in standard tables[36] and the entropy of $SO_3F\cdot$ can be estimated by comparison with similar species. The entropies of the ionic solids can be estimated by taking advantage of an empirical correlation which Bartlett and Mallouk[35,37] observed which relates standard entropies of ionic solids to their molecular volumes according to the linear equation:

3.15) $S°(\text{cal mole}^{-1}\ \text{deg}^{-1}) = 0.44\ V_{\text{molecular vol.}}(Å)$

The molecular volume of $O_2^+SO_3F^-$ can be estimated by noting that O_2^+ has a molecular volume ≈ 2.5 $Å_3$ less than NO^+ in the solid state.

The lattice energy (U) of the ionic solid produced in eqns. 3.12 and 3.13 can similarly be estimated by correlation with its molecular volume as shown by Bartlett and Mallouk:

3.16) $U\ (\text{kcal mole}^{-1}) = 556.3\ V^{-1/3}\ (Å^{-1}) + 26.3$

The ionization energies of O_2 and NO are 278 and 213 kcal mole^{-1} respectively[38]. Hence, by the described method the electron affinity of $SO_3F\cdot$ is estimated to be between 78(5) and 143(5) kcal mole^{-1}. Combining this with the earlier observation that $SO_3F\cdot$ spontaneously intercalates graphite the electron affinity of $SO_3F\cdot$ can be more accurately estimated to be between 120 and 143 kcal mole^{-1}.

2. Extent of Charge Transfer

The extent of charge transfer in (BN)xSO3F was not investigated in the

present research. Not all of the fluorosulfate may exist as the anion, $SO3F^-$, but there could be a significant amount of $S_2O_6F_2$ and even the radical species, $SO3F\cdot$, present. Neutral fluorosulfate could be functioning as dielectric spacers. The stability gained by some $S_2O_6F_2$ or $SO3F\cdot$ functioning as dielectric spacers in shielding the SO_3F^- anions could compensate for the decreased lattice energy associated with the lower sheet and intercalant charges. However, it is unlikely that more than 1/3 of the intercalated species would be neutral since beyond that concentration of neutrals, lattice energy advantages rapidly diminish. The rather low observed conductivity of the $(BN)_3SO_3F$ is therefore probably due to low carrier mobility associated with the heteroatomic character (different sizes of the B p_z and N p_z orbitals). It is probable that the conductivity of pristine $(BN)_3SO_3F$ would be higher than observed here. Clearly the decomposition represented in equation 3.8 must already have been going on before the measurements were made. The extent of the decomposition is not known.

E. Summary

A first-stage boron nitride fluorosulfate salt can be readily prepared with the composition $(BN)_3SO_3F$. This salt has a room temperature specific conductivity approximately 12 orders of magnitude greater than that of the parent BN. $(BN)_3SO_3F$ also exhibits a metallic conductivity dependence upon the temperature.

When subjected to dynamic evacuation the salt undergoes an irreversible thermal decomposition to BN, $S_2O_5F_2$, $NO^+SO_3F^-$ and B_2O_3. At no time has there been any evidence for a higher stage boron nitride fluorosulfate salt.

The c-spacing and composition of $(BN)_3SO_3F$ both support a two-dimensional closed-packed arrangement of the SO_3F^- anions within the BN galleries, with the three-fold axis of the anions aligned parallel to the c-axis of the host lattice. Comparison of the gallery heights for the first-stage graphite and BN fluorosulfate salts combined with evidence for the alignment of the SO_3F^- anion parallel to the host lattice support nestled and un-nestled tetrahedral arrangements for the anions in graphite and BN respectively.

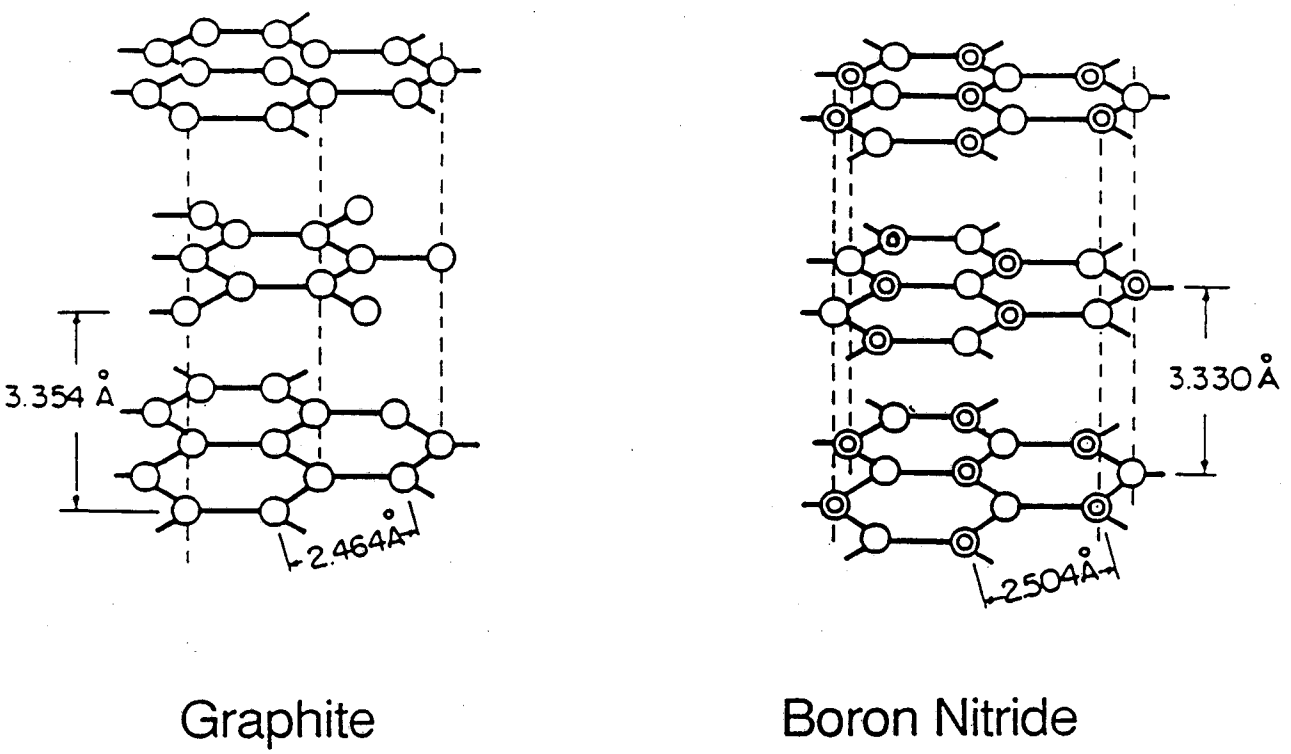

Figure 3.1. Comparison of the layered structures of graphite and boron nitride.

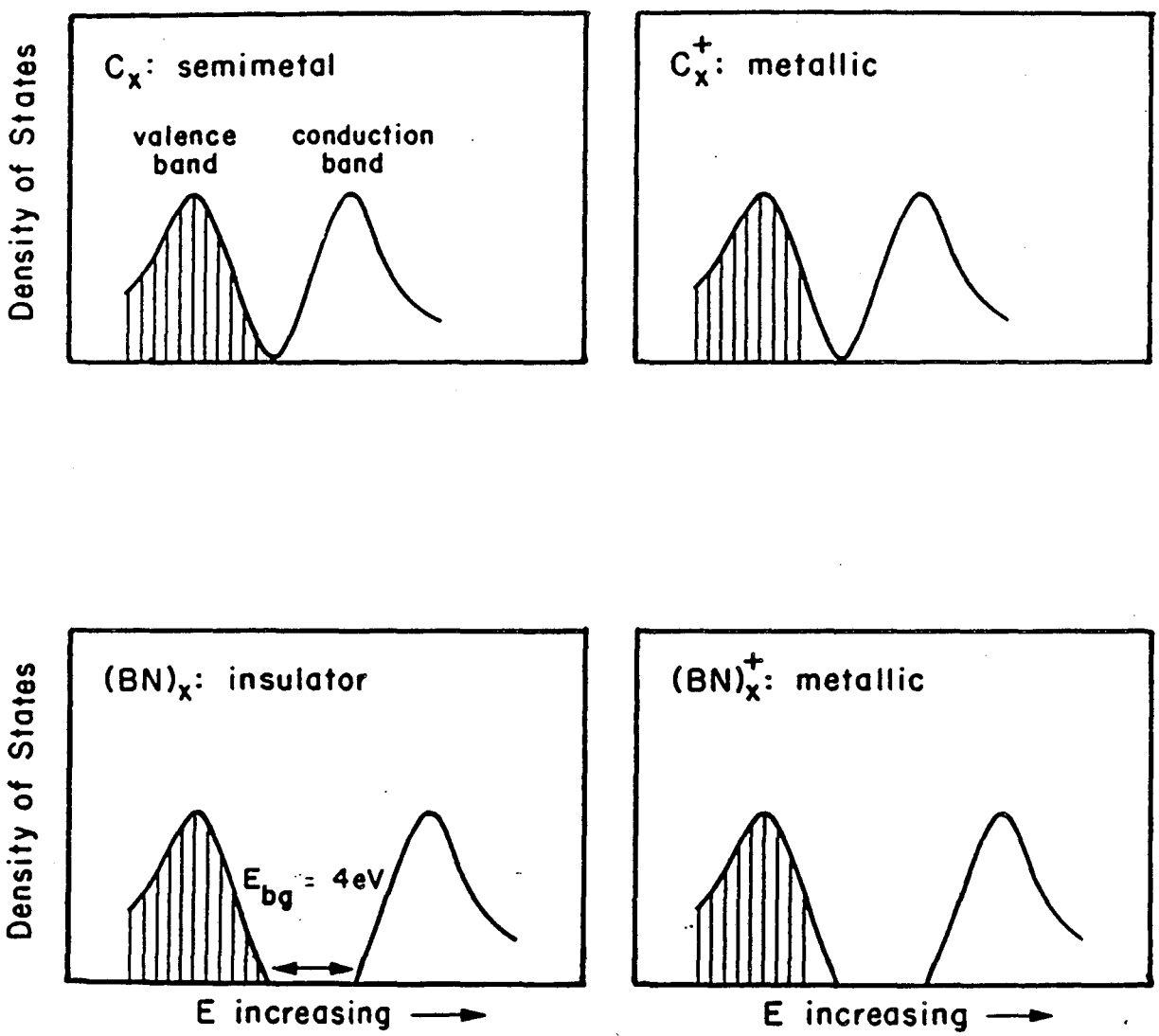

Figure 3.2. Simple band diagram model for pristine graphite and boron nitride and their oxidized states.

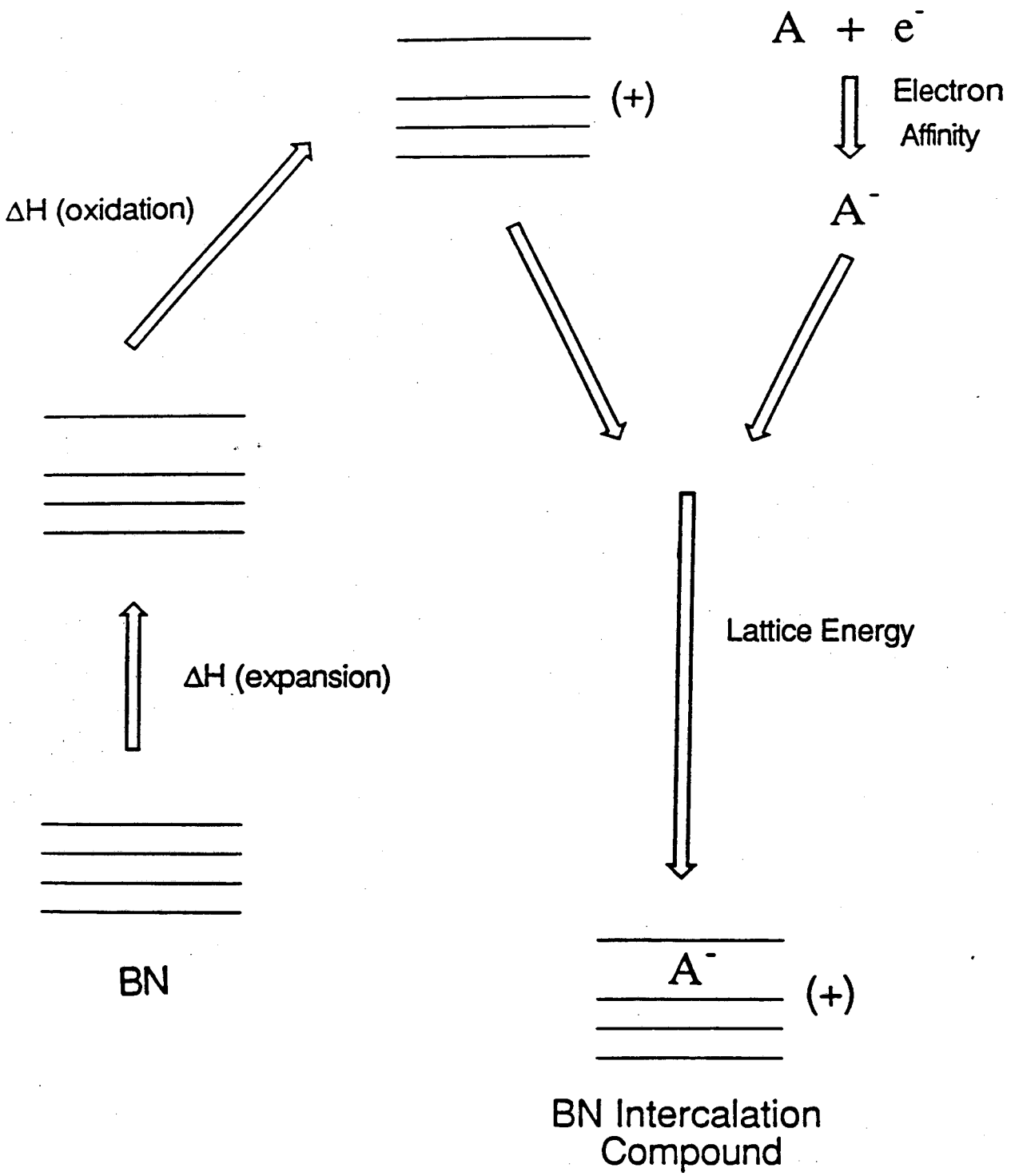

Figure 3.3. Born-Haber cycle for the oxidative intercalation of boron nitride.

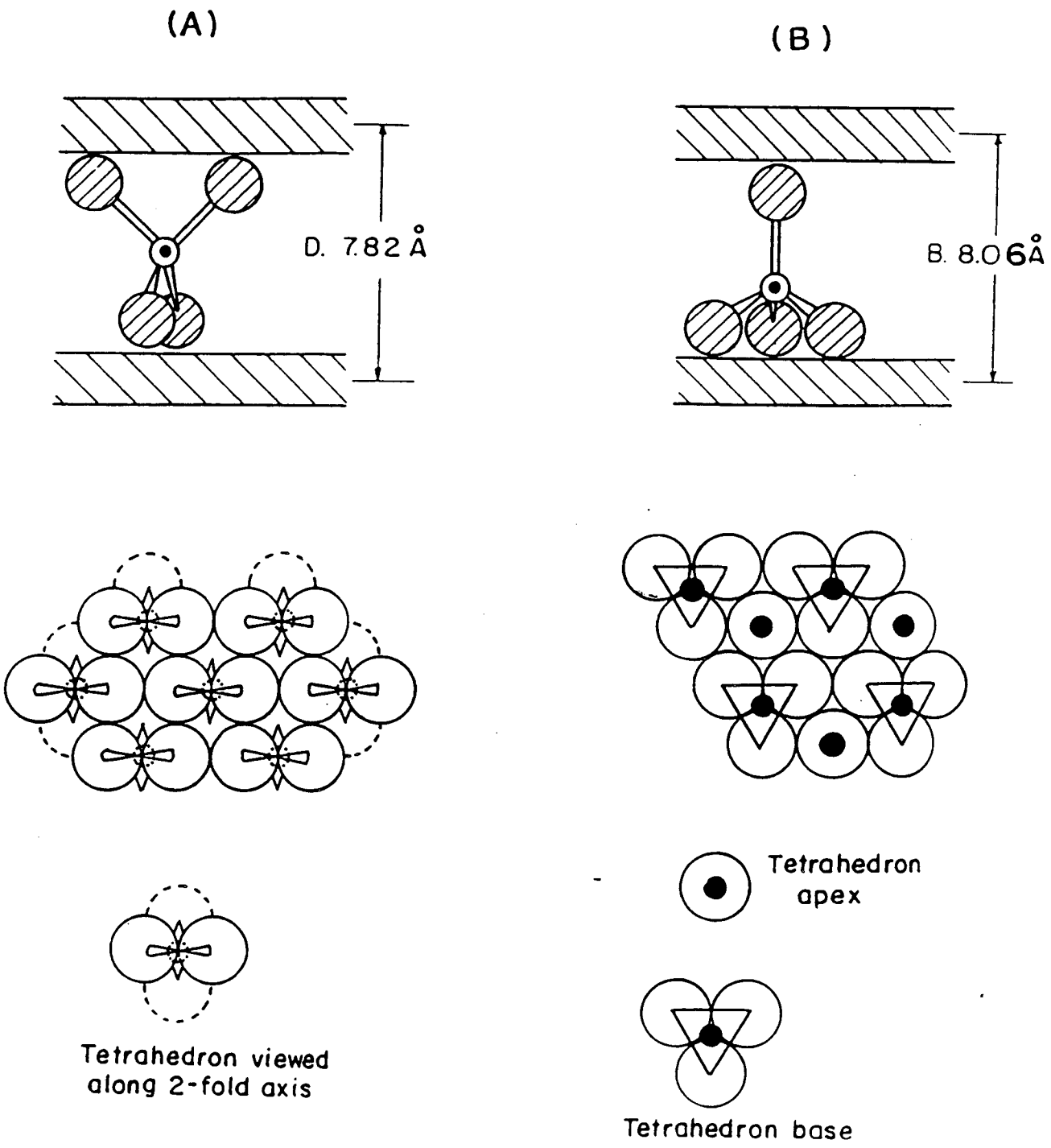

Figure 3.4. Possible arrangement of the SO_3F^- anions within the boron nitride sheets. In orientation "A" the tetrahedral SO_3F^- anion is arranged such that one of its molecular pseudo two-fold axis is aligned parallel to the c-axis of BN; and in "B" a pseudo three-fold axis is parallel to the c-axis of BN.

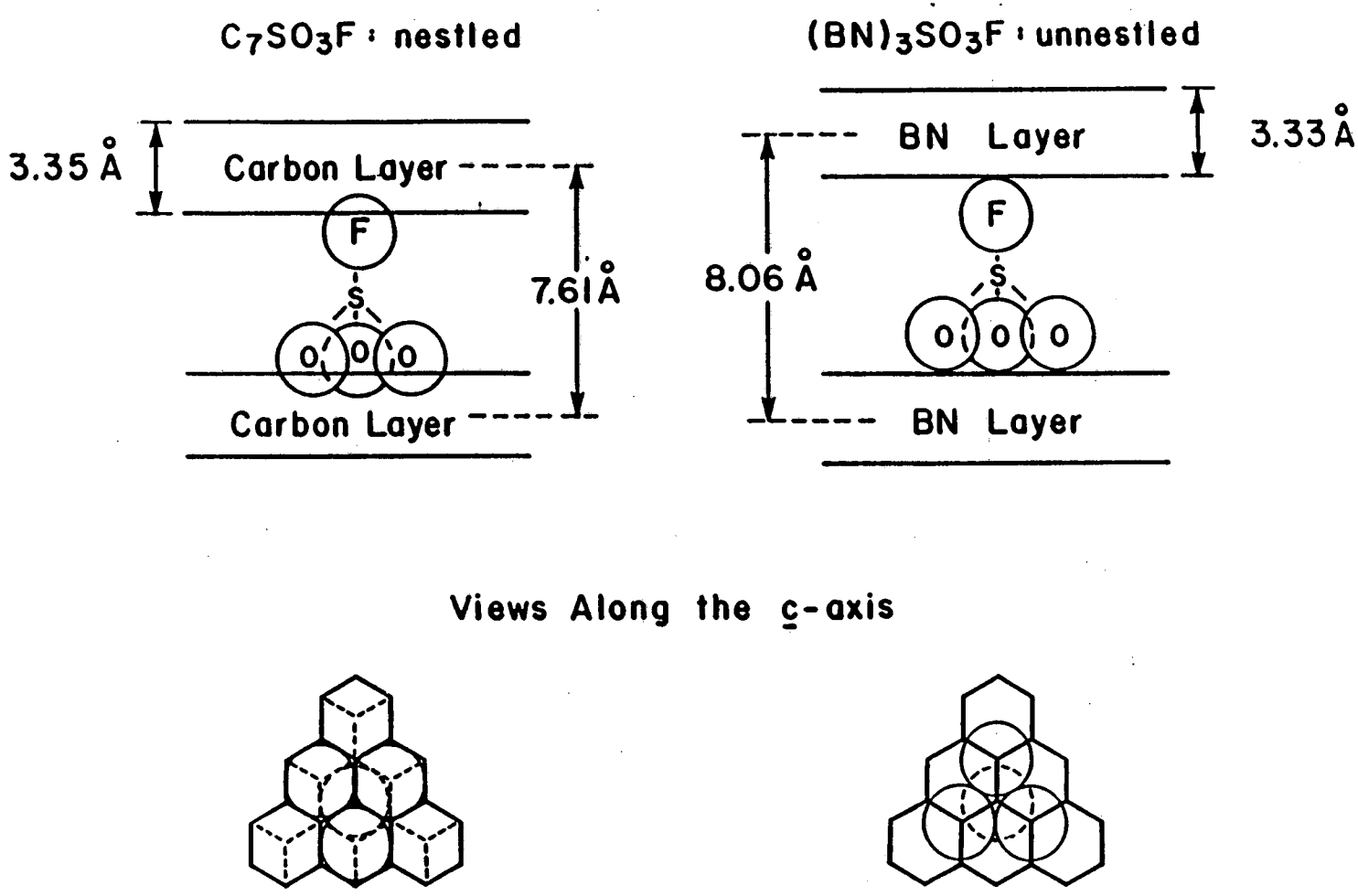

Figure 3.5. Nestled and unnestled models for graphite and boron nitride fluorosulfate.

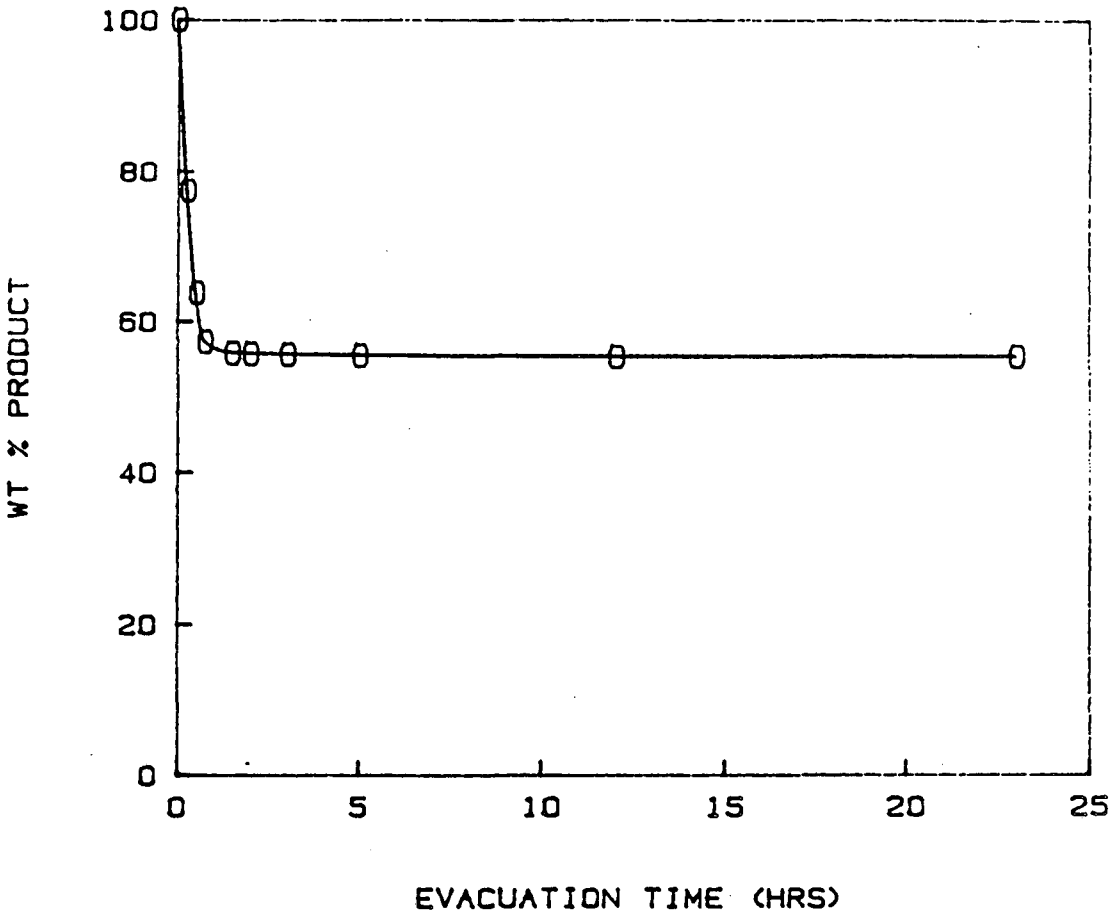

Figure 3.6. Thermal decomposition of $(BN)_{3.0}SO_3F$.

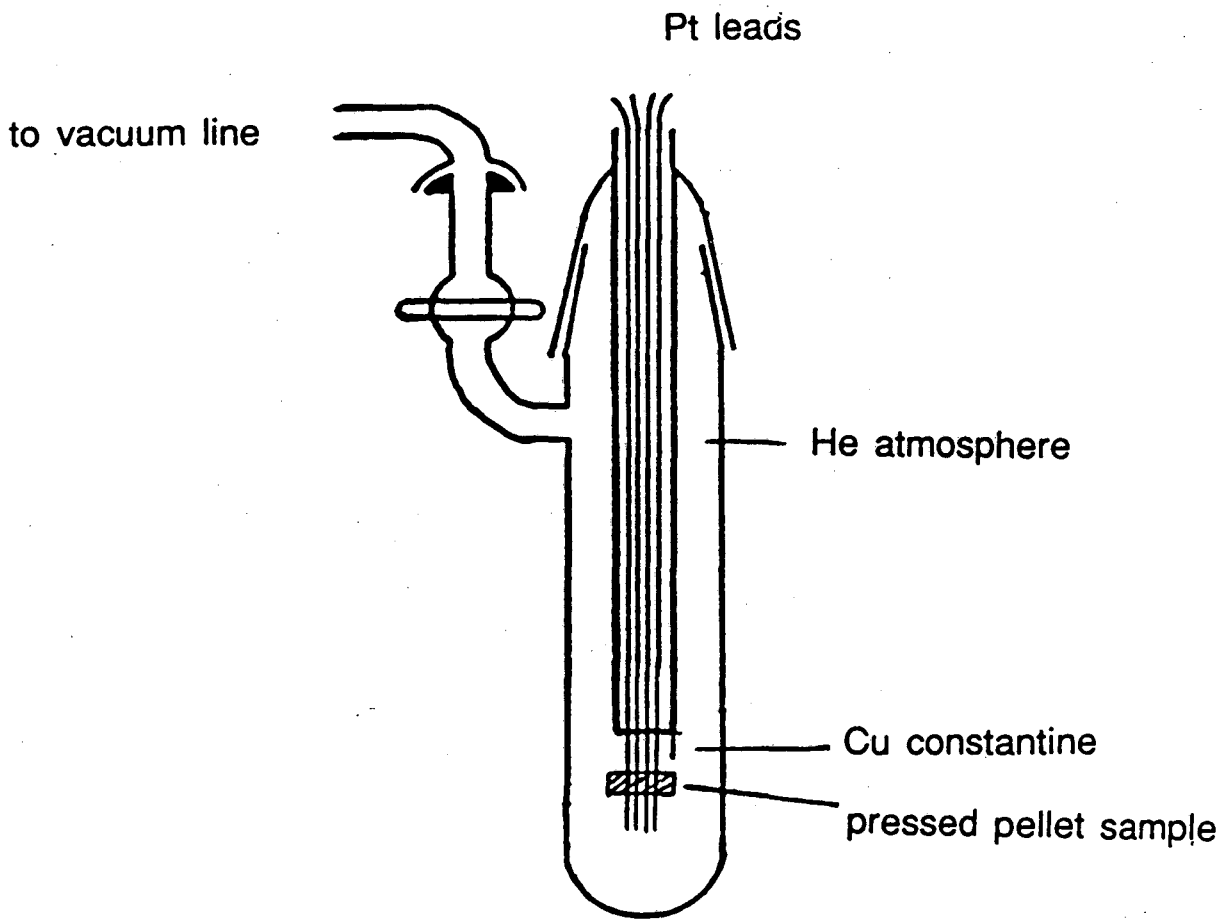

Figure 3.7. Schematic diagram of four-probe electrical conductivity apparatus.

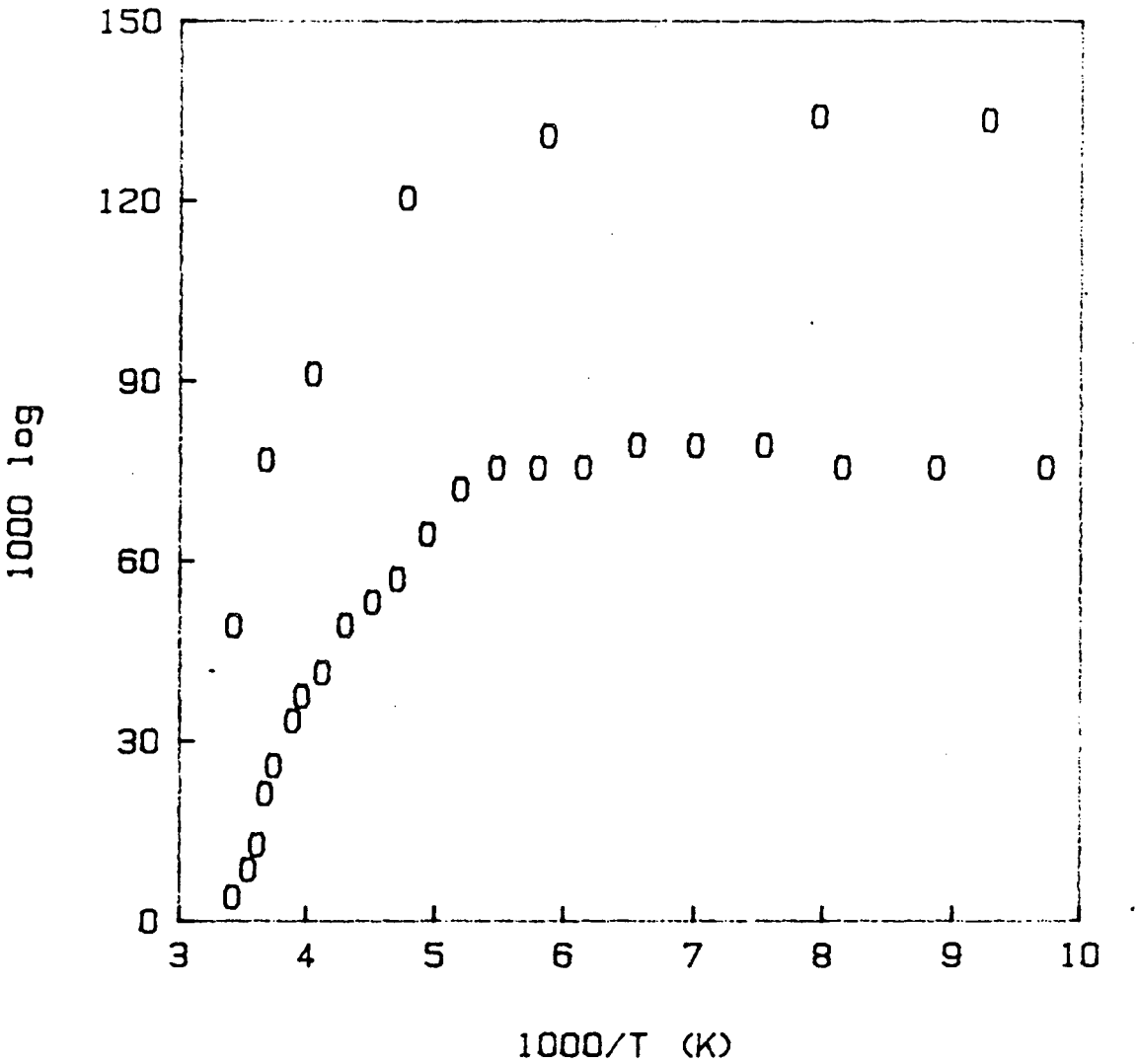

Figure 3.8. Specific electrical conductivity of $(BN)_3SO_3F$ (nominal composition). The boron nitride salt exhibits a metallic conductivity dependence upon the temperature.

Table 3.1. X-ray powder data for $(BN)_3SO_3F$. The observed and calculated $1/d^2$ values with their possible indexing are given below.

$(BN)_3SO_3F$: a = 2.49 Å, c = 8.05(2) Å			
Intensity	*hkl*	$1/d^2$(obs.)	$1/d^2$(calc.)
VS	002	0.0616	0.0618
M	003	0.1378	0.1390
S	100	0.2158	0.2147
M	004	0.2479	0.2471
W	005	0.3830	0.3861
M	110	0.6413	0.6442
VW	111	0.6539	0.6596
VVW	112	0.7054	0.7060
VW	200	0.8564	0.8589
W	210	1.4992	1.5031

Table 3.2a. Gravimetric data and c-spacing for $(BN)_xSO_3F$.

sample	weight BN (mg)	weight product (mg)	"x" in $(BN)_xSO_3F$	c_o (Å)
BN + $S_2O_6F_2$ (*l*):				
	88.6	204.9	3.04	8.07
	101.9	235.3	3.05	8.05
	169.6	365.9	2.92	8.05
	173.3	407.0	2.96	8.06
	193.0	447.9	3.02	8.06
	246.4	578.4	2.96	8.08
BN + $S_2O_6F_2$ (*g*)				
2 hrs:	107.3	211.7	4.11*	
	125.8	230.4	4.80*	
4 hrs:	144.2	330.4	3.09	8.04

* X-ray powder pattern showed mixture of BN and $(BN)_xSO_3F$.

Table 3.2b. Gravimetric data for the thermal decomposition of $(BN)_3SO_3F$ when evacuated.

	initial composition		
	$(BN)_{3.07}SO_3F$	$(BN)_{3.04}SO_3F$	$(BN)_{3.0}SO_3F$
init. wt. (mg):	123.8	249.1	276.3
final wt. (mg) (25 hr evac):	68.4	140.9	150.4
% wt. loss of product†:	44.7	43.4	45.6

† A 43.7% weight reduction of the solid products would be associated with the following rxn:

$$6(BN)_3SO_3F(s) \rightarrow 17BN(s) + 5/2S_2O_5F_2(g) + NOSO_3F + 1/2B_2O_3(s)$$

CHAPTER IV

SOME NEW INTERCALATION COMPOUNDS OF BORON NITRIDE

A. Introduction

Attempts were made to prepare new boron nitride intercalation compounds by two main synthetic routes: (1) by direct interaction of BN with the oxidizing agent(s) and (2) by displacement of the intercalant guest species with another oxidizing agent.

For intercalation by direct reaction a number of oxidizing agents were tried, including several MF_5 Lewis acid species (M = P, As, Sb) and some MF_6 species (M = Os, Ir, Pt). The discussion of the reaction of BN with the hexafluorides will be reserved for the next chapter. As first suggested by Bartlett and his coworkers[39,40] AsF_5 may serve as an oxidizer via the following half-reaction:

4.1) $3MF_5 + 2e^- \rightarrow 2MF_6^- + MF_3$

Similarly, this half-reaction may also apply to PF_5 and SbF_5 as well. The electron affinity of these Lewis acids is thereby quite high. However, in combination with F_2 they have considerably more oxidizing strength, and can act as one-electron oxidizers according to the following half-reaction:

4.2) $MF_5 + 1/2F_2 + e^- \rightarrow MF_6^-$

Hence, the presence of gaseous F_2 permits the complete conversion of MF_5 to MF_6^-. Unfortunately, the marginal stability of BN in the presence of elemental F_2 makes such reactions quite precarious. In instances in which there was some decomposition of BN observed in the presence of MF_5 and F_2 the reaction

temperature was lowered to decrease the amount of decomposition. The free energy change associated with the above half-reactions are shown in table 4.3.

It has been known for some time that graphite will react with the MF_5 species just mentioned to give intercalation compounds. AsF_5 and SbF_5[41] will intercalate graphite either in the presence or absence of F_2, whereas PF_5 requires F_2 to intercalate graphite. By investigating the reaction that BN undergoes with these systems it is possible to make a direct comparison of the intercalation chemistry of BN and graphite.

The displacement reactions may have an energetic advantage over direct intercalation reactions. In order to accommodate the intercalant species a fixed amount of energy (fig. 3.3) must be spent to separate the sheets to overcome the electrostatic and van der Waals attractions between the layers. This sheet separation energy is estimated to be approximately 4 kcal/mole(BN)[42] and would therefore be a significant component of the activation energy for intercalation. However, displacement of an intercalant such as SO_3F by an alternate anion intercalant circumvents that activation energy obstacle.

All of the displacement reactions attempted involve the interaction of $(BN)_3SO_3F$ with various Lewis acids. An ideal quantitative displacement would proceed according to the following net reaction:

4.3) $$SO_3F^- + X \rightarrow SO_3F\cdot + X^-$$

Where X is the oxidizing agent and the anionic species is the intercalant. For a thermodynamically favored reaction it is necessary to select an oxidizing system which has a higher electron affinity than the fluorosulfate radical (see p. 29).

Another consideration has to do with the relative size of the anion of the reacting species and the anion of the displaced species. As the reader will recall, the fluorosulfate anions of $(BN)_3SO_3F$ are believed to comprise a two-

dimensional closed-packed array of tetrahedral anions between enclosing BN layers. Therefore, spacial limitation prohibit a one-for-one displacement of the smaller tetrahedral SO_3F^- anions by the larger octahedral MF_6^- anions (barring a large increase in gallery height), and, consequently, require a decreased charging of the boron nitride sheets. Since the molecular volume of a fluoride is roughly proportional to the number of fluorine atoms in the molecule, and the F and O ligands are compatible, the volume of MF_6^- is approximately 50% greater than the volume of SO_3F^-. Therefore, for every MF_6^- that is incorporated into the salt, 3/2 of an SO_3F^- is displaced:

4.4) $$3(BN)_3^+SO_3F^- + 2MF_5 + F_2 \rightarrow 2(BN)_{4.5}^+MF_6^- + 3SO_3F\cdot$$

However, if there is a significant expansion of the c-spacing accompanying this reaction then a one-for-one displacement may be approached.

The actual displacement reactions observed were far more complicated than eq. 4.4 indicates. As in the boron nitride fluorosulfate system there is some decomposition occurring in the displacement reactions as well. A detailed account of the observed reactions is given in the following sections.

B. Experimental

1. Direct Reactions

Reaction of BN with PF_5 alone and with PF_5/F_2 mixture. Approximately 800 torr of PF_5 was placed over 55 mg of pretreated BN contained in a Pyrex tube. After 2 hours no coloring of the BN was noticed. Gravimetry and X-ray of the product indicated that no intercalation or decomposition of the BN had occurred. In a second experiment 108 mg of BN was placed in a passivated stainless-steel reaction vessel fitted with a Whitey valve. Approximately 2 mmol of PF_5 was condensed into the reaction vessel at -196°C and allowed to warm to ambient temperature (22°C) reaching a total pressure of 10 atmospheres of PF_5. The reaction was allowed to proceed for 6 hours with constant mechanical agitation after which the PF_5 was removed and the reactor assembly transferred into the Dri-lab. The white product, weighing 107 mg, was shown by X-ray to be unreacted BN.

In a similar experiment 94 mg of BN was exposed to a 2:1 gaseous mixture of PF_5/F_2 and allowed to react at room temperature for 5 hours. Following reaction the volatiles over the solid product were expanded into an IR cell and shown to be predominantly PF_5 with a trace amount of BF_3. The product weighed 89 mg and the X-ray analysis showed it to be crystalline BN. The reaction was repeated at 0°C for 5 hours in an attempt to avoid decomposition of BN. No evidence of BF_3 was detected by infra-red analysis of the volatiles and gravimetry indicated >99% recovery of BN following treatment with PF_5 and F_2.

Reaction of BN with AsF_5 alone and with AsF_5/F_2 mixture. Pretreated BN was exposed to 12 atmospheres of AsF_5 at room temperature and allowed to react for 14 hours. Examination of the product revealed only BN with no evidence of decomposition. This reaction was repeated with 20 atmospheres of AsF_5 for 4 hours. The BN was recovered quantitatively with no evidence of intercalation or decomposition.

To increase the oxidizing capability of the system BN was treated with 12 atmospheres of a 2:1 gaseous mixture of AsF_5/F_2. The reaction vessel was held at 0°C and allowed to react for 6 hours. Approximately 97% of the BN was recovered with no indication of intercalation. In a similar experiment BN was exposed to 12 atmospheres of a gaseous mixture of AsF_5/F_2 at ambient temperature and allowed to react for 7 days after which the volatiles were removed and the sample brought into the Dri-lab. The colorless product was shown by X-ray powder diffraction to be BN.

Reaction of BN with $O_2^+AsF_6^-$. 53 mg of BN (2.13 mmol) and 230 mg of $O_2^+AsF_6^-$ (1.04 mmol) were placed in a stainless-steel reaction tube in the Dri-lab. The white powders were intimately mixed with no visible indication of reaction. A Whitey valve was attached to the tube and the assembly was removed from the Dri-lab. The reactor was placed on a mechanical agitator for 24 hours then removed and transferred into the Dri-lab. The solid product remained colorless having a composite weight of 282 mg. X-ray analysis indicated that no chemical reaction had occurred. Subsequently, the reaction tube was placed in a sand bath at 150°C for 3 hours. A significant amount of BF_3 was observed in the IR of the expanded volatiles, however no intercalation compound or decomposition

products were observed in the X-ray powder pattern.

Reaction of BN with SbF_5 alone and with Sb_5/F_2 mixture. An excess of freshly distilled SbF_5 was placed dropwise onto pretreated BN in the Dri-lab. No reaction occurred at ambient temperature nor upon warming to 90°C in an oil bath. The SbF_5 was removed by dynamic evacuation leaving behind a white BN product with a pasty consistency, presumable wet with SbF_5.

The above reaction was repeated with the addition of F_2 to increase the oxidizing power. BN and SbF_5 were placed in a 3:1 molar ratio into a stainless-steel reaction tube. The tube was fitted with a valve and removed from the Dri-lab. F_2 was condensed into the reaction tube at -196°C such that the ratio of the SbF_5 to F_2 was 2:1. The reactor was allowed to warm to 0°C. After 6 hours the residual F_2 was removed at -196°C and the less volatile gases were expanded into an IR cell at room temperature. A small amount of BF_3 was present in the volatiles. The product was a pasty, light blue material, less colored than the $(BN)_3SO_3F$ compound described in the previous chapter. The X-ray pattern of the products showed the (002) reflection of an intercalated BN, corresponding to $\underline{c}$ = 8.01 Å as well as some unreacted BN residue. The gravimetry showed a weight increase over the unreacted BN, but limits on the composition could not be satisfactorily assigned due to the incompleteness of the reaction and the observed decomposition.

The above reaction of BN with SbF_5/F_2 was repeated several times with similar results. In an effort to reduce decomposition the reaction was run at -23°C in a $CCl_4/N_2(l)$ slush bath. In this instance no evolution of BF_3 was detected, however, the product was a paler blue perhaps indicative of a less extensively oxidized system.

Reaction of BN with $AsF_5/S_2O_6F_2$ system. Several attempts were made to oxidize BN with a liquid mixture of AsF_5 and $S_2O_6F_2$. Pure AsF_5 has a vapor pressure of ≈ 25 atmospheres at room temperature, while $S_2O_6F_2$ has a much lower vapor pressure of ≈ 0.2 atmospheres. Glass and Teflon apparatus were used preferentially to stainless-steel because of the possible attack of the powerfully oxidizing liquid mixture of $AsF_5/S_2O_6F_2$ on the metal surface. To avoid subjecting the glass or Teflon apparatus to excessive pressure two reactions schemes were employed: (1) a low temperature reaction (-56°C) where both AsF_5 and $S_2O_6F_2$ are low volatility liquids, and (2) a room temperature reaction in which the apparatus was placed in a bomb then slowly pressurized to counter-balance the pressure within the reaction vessel.

For the low temperature reaction a 1/2" o.d. Teflon U-tube was drawn out to ≈ 1/4" at the base and equipped with a Teflon side-arm via a Teflon "T" connection. The ends of the U-tube were capped with Whitey valves. The vessel was passivated with $S_2O_6F_2$ and AsF_5 and transferred into the Dri-lab where BN was loaded into the side-arm. The assembly was removed from the Dri-lab and AsF_5 was distilled into the U-tube at -78°C. BN was transferred onto the AsF_5 liquid in the base of the U-tube by inverting the side-arm. $S_2O_6F_2$ was subsequently condensed into the opposite side of the U-tube while maintaining the assembly at -78°C. The system was warmed to -56°C [octane/N_2(*l*)] and reaction allowed to procede for 2-3 hours. The liquids appeared to be miscible with no noticeable coloration, suggesting that there was no significant concentration of radical species at this temperature. The BN remained colorless during the course of the study. The $AsF_5/S_2O_6F_2$ mixture was removed by evacuation at -56°C leaving behind a white/pale blue solid for which

the X-ray powder pattern showed only BN.

An all-glass apparatus was used for the room temperature reaction run in a pressurized bomb. The apparatus consisted of a 4" length of 3/8" o.d. glass tubing adapted to 1/4" on either side and equipped with a break-seal in the center. The glass vessel was transferred into the Dri-lab and BN was placed in one side, then capped with a Whitey valve. The assembly was removed from the Dri-lab and AsF_5 and $S_2O_6F_2$ were successively condensed into the vessel at -196°C in the molar ratio of 2:1. While holding the reactor at -196°C it was sealed under vacuum just beneath the valve with a gas-oxygen flame. The sealed tube was transferred while cold into a Monel bomb and gradually pressurized with N_2 gas over a 5 minute period to a total of 12 atmospheres, minimizing the pressure felt by the glass apparatus. After 12 hours of reaction at ambient temperature the bomb was again cooled to -196°C, evacuated and re-opened to remove the glass vessel, to which a Whitey valve was attached to the chamber opposite the break-seal. The seal was broken and the excess liquid was removed by evacuation at -78°C. The majority of the solid product was colorless with a small amount of dark blue solid concentrated in the tip of the break seal. The white material was shown by X-ray to be poorly crystalline BN while attempts to analyze the blue solid were unsuccessful due the limited quantity of material.

Recognizing that AsF_5 might be quite soluble in $S_2O_6F_2$, or, may react with the peroxide to give $AsF_5SO_3F\cdot$ radical, which in either case, would reduce the vapor pressure of the system, the two liquids were condensed into a 1/2" Teflon-FEP tube and allowed to slowly warm to monitor the vapor pressure. The vapor pressure of a 2:1 liquid mixture of $AsF_5/S_2O_6F_2$ was observed to be 820 and 1040 torr, respectively, at 0°C and 22°C. The liquids formed a miscible, faint

yellow solution at ambient temperature.

In a follow-up experiment BN was loaded into a Teflon-FEP tube containing a Teflon stirrer-bar in the Dri-lab and fitted with a Whitey valve. The reaction vessel was transferred out of the Dri-lab where AsF_5 and $S_2O_6F_2$ were distilled into the reactor at -196°C in the molar ratio of 2:1. The reaction tube was warmed to -78°C and briefly stirred to obtain a homogenous liquid mixture above the colorless solid. The CO_2/acetone bath was removed, allowing the sample to slowly warm to ambient temperature. Within a few minutes the solid changed from colorless to grey to dark blue. The product was vented to 0 torr and an X-ray powder pattern was taken showing a first-stage salt with a c-spacing of 8.26 Å, very similar to the powder pattern obtained from the reaction of $(BN)_3SO_3F$ with AsF_5 described in the next section.

2. **Displacement Reactions**

Boron Nitride Hexafluoroarsenate. Pretreated BN was placed in a passivated stainless steel reactor and exposed to an excess of $S_2O_6F_2$ (*l*) at room temperature for one hour. The excess peroxide was removed by evacuation and the system was vented to 0 torr. Brief dynamic evacuation yielded a blue salt of the composition $(BN)_{3.1}SO_3F$. A powder pattern of the material was taken showing a first stage salt with no residual BN. AsF_5 and F_2 were condensed into the reaction vessel at 77 K then allowed to warm to room temperature providing approximately 8 atmospheres of a 2:1 gaseous mixture of AsF_5/F_2 over the salt. After 2 hours of reaction the volatiles over the sample were expanded into an IR cell revealing a mixture of AsF_5 and $S_2O_5F_2$ and a small amount of BF_3. The sample was cycled two more times with AsF_5/F_2 under similar conditions. After the second cycle a relatively small amount of displaced $S_2O_5F_2$

was observed in the IR spectrum, and after the third cycle no sulfur oxyfluoride species were seen, suggesting that displacement was complete. This series of reactions was repeated several times giving quite similar results. However, in some experiments 3 cycles of AsF_5/F_2 were necessary to completely displace the sulfur oxyfluoride species. X-ray powder patterns of the product consistently showed a first stage salt with a c-spacing of 8.18(2) Å (table 4.1). The room temperature electrical conductivity of the salt was 0.08(2) ohm^{-1} cm^{-1} which was virtually independent of temperature (fig. 4.1). In all cases the resulting product is a blue-black material which is indefinitely stable in a sealed capillary. An upper limit of $(BN)_{4.8}AsF_6$ can be assisgned to the composition by gravimetric analysis. The salt appeared to be thermally stable at 100°C with no detectable gas evolution. Details concerning the experimental results and their interpretation are given in the next section.

Reaction of $(BN)_3SO_3F$ with AsF_5. Boron nitride fluorosulfate was prepared in a stainless-steel reactor in the manner previously described. Approximately 8 atmospheres of AsF_5 was placed over this blue salt and allowed to react for several hours on a mechanical vibrator. An IR of the volatile gas showed AsF_5 and a significant amount of displaced $S_2O_5F_2$. A second treatment with AsF_5 showed a small amount of displaced $S_2O_5F_2$ in the volatiles and a third cycle showed none, indicating that displacement was complete. This experiment was repeated several times giving similar results. However, it was noticed that if a smaller sample size of $(BN)_3SO_3F$ was used, or if the pressure of AsF_5 was increased the displacement was complete in one cycle. In all cases there was no evidence of $S_2O_6F_2$ displacement. The dark blue product was shown by X-ray to be a first-stage salt with a c-spacing of 8.25(2)Å (table 4.2). The ambient

temperature electrical conductivity was 1.5 ohm^{-1} cm^{-1} which increased by a factor of ≈ 2 as the temperature was lowered to 100 K (fig. 4.1b). An upper limit to the composition of $(BN)_{>9}AsF_5SO_3F$ was assigned by gravimetry. A thermal study showed the salt to be stable up to 100°C. See the next section for details.

C. Results

Of all of the direct reactions of BN with Lewis acids only SbF_5 in combination with F_2 gave an intercalation compound. The c-spacing of the light blue first-stage salt is 8.01(2) Å. The decreased coloration of this salt relative to $(BN)_3SO_3F$ was interpreted as the BN network being less highly oxidized due to the tendency of antimony (V) fluorides to form polymeric anions. Unfortunately SbF_5 will only oxidize BN in the presence of F_2, therefore, the intercalation reaction is complicated by the oxidative decomposition of BN by molecular fluorine[11]. Calibration of an IR cell for BF_3 indicated that 10(3) % of the original BN underwent decomposition to BF_3 and presumably N_2 (no nitrogen fluoride species were seen in the IR of the volatiles). The boron nitride fluoroantimonate salt was not vacuum stable, therefore, gravimetric attempts to determine the composition of the salt by evacuation of excess SbF_5 were unsuccessful, yielding a colorless pasty material.

Several displacement reactions were effective in synthesizing new BN compounds. $(BN)_3SO_3F$ interacted with AsF_5 and F_2 to give a blue-black first-stage intercalation compound of with a c-spacing of 8.19(2) Å. Generally, two successive treatments with AsF_5/F_2 were sufficient to completely displace the sulfur oxyfluoride species of $(BN)_3SO_3F$. A displacement involving a simple redox reaction might proceed according to the following equation:

$$4.5) \quad 3(BN)_3SO_3F + 2AsF_5 + F_2 \rightarrow 2(BN)_{4.5}AsF_6 + 3SO_3F\cdot$$

However, examination of the volatiles products over the reaction by expansion into an IR cell consistently showed $S_2O_5F_2$ as the only displaced sulfur oxyfluoride species. Oxygen was being incorporated into the solid product as in the case of the thermal decomposition of $(BN)_3SO_3F$ discussed in the previous

chapter. Careful examination of the X-ray powder patterns of the product showed a weak cubic pattern corresponding to $NO^+AsF_6^-$, paralleling the NO^+ salt formation observed in the decomposition products of $(BN)_3SO_3F$. Therefore, a more accurate formulation of the observed reaction might be:

$$4.6) \quad (BN)_xSO_3F + AsF_5 + 1/2F_2 \rightarrow (BN)_yAsF_6 + S_2O_5F_2 + NO^+AsF_6^- + BF_3$$

The above equation is not balanced in view of the ongoing decomposition of the boron nitride salt. This is consistent with the observation that the $NO^+AsF_6^-$ pattern in the X-ray became more prevalent and the overall weight of the product increased with continued treatment with AsF_5 and F_2. This ongoing decomposition to a nonvolatile impurity made it difficult to determine the true composition of the salt by gravimetry. However, by obtaining the weight of the boron nitride fluoroarsenate product immediately after all of the sulfur oxyfluorides are displaced (two cycles with AsF_5/F_2) it was possible to assign an upper limit to the fluoroarsenate content of the salt. If one assumes that $(BN)_yAsF_6$ is the only solid product formed in the displacement reaction after two cycles with AsF_5/F_2 then y can be estimated as $\approx 4.8(4)$. Since $NO^+AsF_6^-$ has been detected in the solid product we can say that some of the weight gain must be due to NO^+ salt formation and hence $y > 4.8(4)$.

Four-probe conductivity measurements were made on pressed pellets of $(BN)_yAsF_6$. The room temperature specific conductivity was measured to be 0.08 $ohm^{-1}\ cm^{-1}$. The conductivity showed no strong temperature dependence remaining almost constant as the temperature was lowered to $\approx$ 100 K (see fig. 4.1a). The conductivity of this salt was measured to be a factor of 15 less conducting than $(BN)_3SO_3F$. This reduced conductivity may be due to the partial fluorination of the boron nitride sheets by elemental fluorine which may localize

charge and reduce the electron mobility. Such decreased conductivity behavior was observed by Bartlett and Mallouk[43] in C_xF salts ($2 \geq x \geq 3$) which was attributed to the localization of π electrons of graphite due to the fluorination of the graphite sheets.

As mentioned in the experimental section, BN does not give an intercalation compound with AsF_5 and F_2, however, the displacement reaction of $(BN)_3SO_3F$ with AsF_5 and F_2 does occur. The direct intercalation of BN by AsF_5 and F_2 might be kinetically hindered, whereas the displacement reaction may be kineticlly feasible due to the decreased activation energy. The lower activation energy of the displacement reaction is the result of energy having already been spent to separate the BN sheets to accommodate the intercalant guest species.

Boron nitride fluorosulfate reacts with excess gaseous AsF_5 to give $(BN)_zAsF_5SO_3F$. The measured c-spacing was 8.25(2) Å which is consistent with the larger anion size. The only displaced sulfur oxyfluoride species seen in the IR of the volatiles was $S_2O_5F_2$, which again indicated that some decomposition was occurring. Noting that NO^+ salts account for some of the weight of the solid product an upper limit can be assigned for the composition of the BN salt: $(BN)_{>9}AsF_5SO_3F$. The ambient temperature specific conductivity of this salt was measured to be 1.5 ohm^{-1} cm^{-1} and showed a small metallic temperature dependence, increasing by a factor of almost 2 as the temperature was lowered to 100 K (fig. 4.1b). This conductivity value is comparable to that observed for $(BN)_3SO_3F$. The conductivity, although having a metallic temperature dependence, is quite low which may be due in part to the high contact resistance of the polycrystalline particles in the pressed pellet, or perhaps due to less conductive NO^+ salt impurities mixed in with the product.

Aubke and coworkers[44] studied an analogous series of reactions utilizing C_xSO_3F instead of $(BN)_xSO_3F$. They claim to have prepared $C_{14}^+(AsF_5SO_3F)^-$ from the interaction of C_7SO_3F with gaseous AsF_5. The resulting salt is a dark blue first-stage compound with a reported c-spacing of 7.92 Å which represents an increase of approximately 0.2 Å over C_7SO_3F. Observations with the BN system are consistent with this, the c-spacing of $(BN)_z(AsF_5SO_3F)$ being 0.19(2) Å greater than $(BN)_3SO_3F$. Aubke reports a high basal-plane conductivity of $\approx 2 \times 10^5$ ohm^{-1} cm^{-1} for $C_{14}^+(AsF_5SO_3F)^-$ and describes it as having limited thermal stability, with the onset of decomposition occurring at 40°C. The relatively high specific conductivity as well as the thermal instability are properties also observed for $(BN)_z(AsF_5SO_3F)$.

D. Summary

Boron nitride will react with SbF_5 and F_2 to give a pale blue first-stage intercalation compound with a c-spacing of 8.01(2) Å. The compound decomposes when subjected to a dynamic evacuation giving a colorless pasty material. Reaction of $(BN)_3SO_3F$ with a gaseous mixture of AsF_5 and F_2 produces a dark blue compound with the composition $(BN)_{>4.8}AsF_6$. The compound is invariably first-stage with a c-spacing of 8.20(2) Å. This material has a room temperature specific conductivity of 0.08 ohm^{-1} cm^{-1} which doesn't vary significantly with temperature (100 K < T < 293 K). This compound is not thermally stable as shown by the principle displaced volatile species as $S_2O_5F_2$, and the formation of $NO^+AsF_6^-$ among the solid products.

Reaction of $(BN)_3SO_3F$ with AsF_5 alone gives the dark blue salt, $(BN)_{>9}AsF_5SO_3F$, with a c-spacing of 8.25(2) Å. It has an ambient temperature conductivity value of 1.5 ohm^{-1} cm^{-1} which is comparable to the conductivity of $(BN)_3SO_3F$. It also exhibits a metallic conductivity dependence upon the temperature. The presence of NO^+ salts was not detected in this study; however, their formation is anticipated by virtue of $S_2O_5F_2$ being the only evolved sulfur oxyfluoride species.

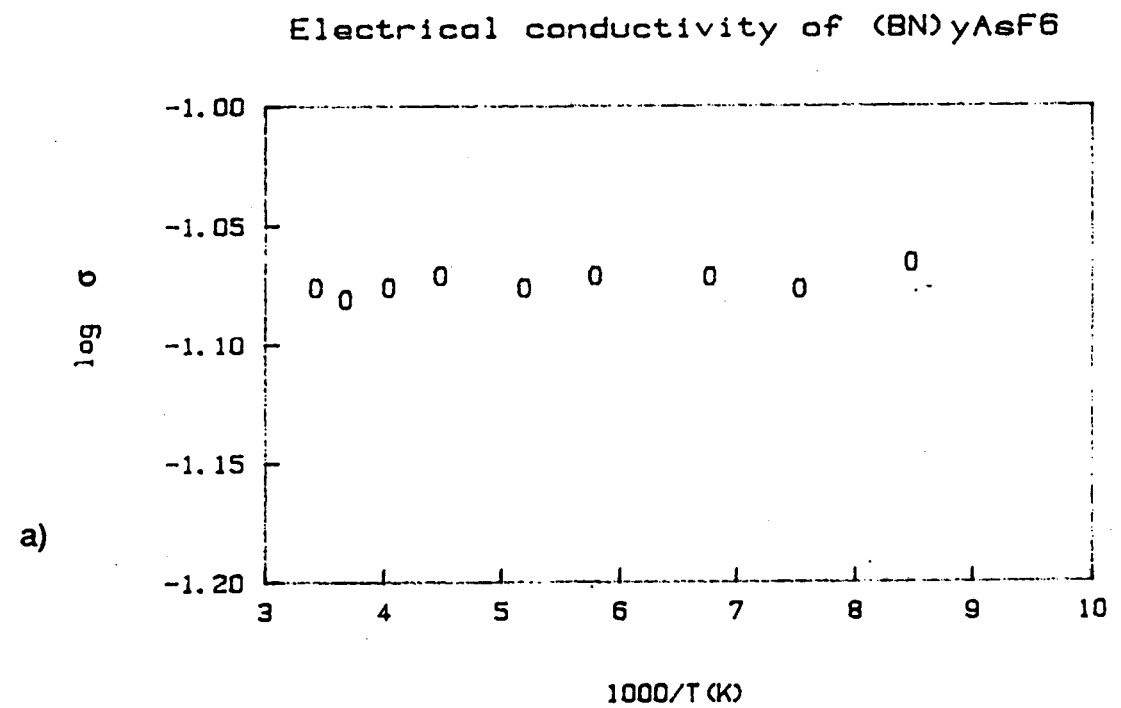

a)

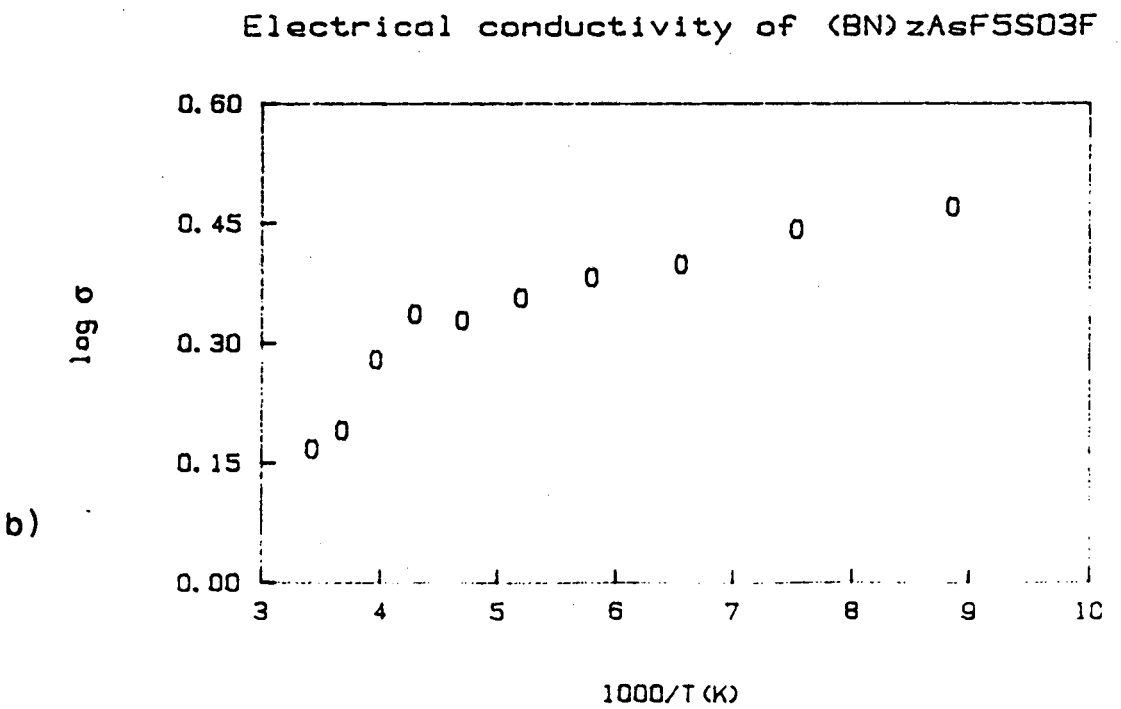

b)

Figure 4.1. Temperature dependent electrical conductivity of $(BN)_yAsF_6$ and $(BN)_zAsF_5SO_3F$. The conductivity of $(BN)_yAsF_6$ remains essentially constant ($\approx$ 0.08 ohm^{-1} cm^{-1}) as the temperature is varied. The conductivity of $(BN)_zAsF_5SO_3F$ increases by a factor of 2 as the temperature is dropped from 293 K (1.5 ohm^{-1} cm^{-1}) to 120 K (2.9 ohm^{-1} cm^{-1}).

Table 4.1. Representative X-ray powder data for $(BN)_xAsF_6$. The observed and calcuted $1/d^2$ values are shown below with their assigned indexing.

$(BN)_yAsF_6$: a = 2.50 Å, c = 8.18(3) Å

Intensity	(*hkl*)	$1/d^2$(obs)	$1/d^2$(calc)
M	001	0.0147	0.0150
S	002	0.0597	0.0598
M	003	0.1350	0.1346
M	100	0.2144	0.2136
WM	004	0.2392	0.2393
WM	110	0.6406	0.6408

Table 4.2 X-ray powder data for $(BN)_2AsF_5SO_3F$. Below are given the observed and calculated $1/d^2$ values with with their possible indexing.

$(BN)_2AsF_5SO_3F$: a = 2.49 Å, b = 8.25(3) Å

Intensity	(*hkl*)	$1/d^2$(obs)	$1/d^2$(calc)
M	001	0.0145	0.0147
S	002	0.0589	0.0588
M	003	0.1322	0.1324
M	100	0.2163	0.2136
WM	004	0.2355	0.2353
WM	110	0.6402	0.6409
WM	111	0.6560	0.6566
W	112	0.6993	0.6998

Table 4.3. Enthalpy changes for for the electron oxidation by MF_5 (M = P, As, Sb) and MF_6 (M = Os, Ir, Pt). All values are given in kcal $mole^{-1}$.

Enthalpy changes for electron oxidation by MF_5 (M = P, As, Sb)

	P	As	Sb
$MF_5(g) + 1/2F_2 + e^- \rightarrow MF_6^-(g)$ [45]	158	170	193
$3/2MF_5(g) + e^- \rightarrow MF_6^- + 1/2MF_3(g)$ [45]	82	121	148

Enthalpy changes for electron oxidation by MF_6 (M = Os, Ir, Pt)

	Os	Ir	Pt
$MF_6(g) + e^- \rightarrow MF_6^-(g)$ [45]	135	161	198

CHAPTER V

THE INTERACTION OF BN WITH MF_6 (Os, Ir, Pt)

A. Introduction

The interaction of BN with various MF_6 (M = Os, Ir, Pt) species was investigated in an attempt to prepare oxidized BN salts. By exposing graphite to ≈ 100 torr vapor pressure of these noble metal hexafluorides one readily obtains dark blue first-stage salts of the limiting composition $C_8^+MF_6^-$ for M = Os, Ir and $C_{12}^{+2}MF_6^{-2}$ for M = Pt[46]. The extent of electron transfer in these salts was evaluated by magnetic susceptibility measurements. A reductive half-reaction involved in the preparation of all three salts is shown below:

5.1) $MF_6 + e^- \rightarrow MF_6^-$

However, in the case of PtF_6 the second electron affinity is large enough to stabilize a two electron transfer, resulting in a more highly charged graphite sheet intercalated with the dianionic species PtF_6^{-2}. The greater coulombic attraction between the graphite sheets and the guest species was given as the explanation for the lower c-spacing of ≈ 7.54 Å for $C_{12}^{+2}PtF_6^{-2}$ as compared to the c-spacing of ≈ 8.06 Å for the corresponding salts of Os and Ir, but at that time nestling of the MF_6^{-2} in the graphite sheets was not considered. That is the likely explanation for the small gallery height. Higher stage salts were successfully obtained by lowering the reaction pressure or temperature.

In view of the estimated electron affinities for these hexafluorides (see table 4.3) one would anticipate that they would have enough energy to withdraw an electron from the BN sheets. However, as mentioned earlier, BN has limited stability with respect to fluorine[15]. Therefore, a concern with these reactions was

the possible decomposition of BN via fluorination rather than the oxidative intercalation of BN. A detailed account of the experiments run and the results obtained are given in the following sections.

B. **Experimental**

Preparation of MF_6. Iridium hexafluoride was prepared by the direct fluorination of the metal. Approximately 1 g of iridium metal was placed in a pre-passivated Monel can (vol. ≈ 100 ml) in the Dri-lab. The can was attached to the vacuum line and F_2 was tensimetrically condensed in to give a total pressure of ≈ 15 atm at room temperature. The loaded can was heated in a sand bath to approximately 250 - 300°C overnight, after which the unreacted F_2 was removed by evacuation at -196°C. The solid volatile product was shown by IR to be IrF_6.

The OsF_6 was prepared in a similar manner with the exception that the metallic osmium was reduced in a H_2 flame prior to treatment with F_2. This precaution was taken to avoid the production of stable osmium oxyfluoride species. PtF_6 had been prepared by a previous worker in this laboratory also by high temperature fluorination.

Interaction of BN with OsF_6. Approximately 2 mmol of BN were placed in a Teflon-FEP tube in the Dri-lab and fitted with a stainless-steel Whitey valve via a Swagelok compression fitting. The reaction vessel was removed from the Dri-lab and attached to a vacuum line where ≈ 1 mmol of OsF_6 was tensimetrically transferred onto the white solid at -196°C. The Teflon tube was allowed to warm to ambient temperature while agitating with a fan. Well below room temperature the yellow OsF_6 could be seen condensed on the wall of the reactor with the colorless BN at the base of the tube. As the vessel warmed over a

period of about 2 minutes the BN powder changed progressively from colorless to light blue to dark blue, then ignited, resulting in a dark gray powder. The X-ray pattern of the product showed predominantly elemental Os, and a very weak pattern attributed to OsF_5. An IR of the gaseous products showed only BF_3.

In an attempt to control the reduction of the OsF_6 another experiment was run in which the reaction temperature was carefully controlled. OsF_6 was condensed onto the BN in a Teflon-FEP tube and allowed to warm to -23°C [$CCl_4/N_2(l)$]. A slight greenish coloration of the BN was observed after 1 hour. The vessel was warmed to 0°C and allowed to react for an additional hour. The dark green colored product was loaded into an X-ray capillary where it was shown to be predominantly OsF_5 with no indication of a lower osmium fluoride.

Interaction of BN with IrF_6. Powdered BN was placed in a sapphire tube in the Dri-lab and fitted with a stainless-steel Whitey valve. IrF_6 was condensed into the reactor at -196°C and allowed to slowly warm to ambient temperature. An exothermic reaction resulted yielding a dark gray product. An IR of the evolved gases showed BF_3 and the X-ray powder pattern of the product showed a strong Ir metal pattern.

This experiment was repeated several times using an excess of IrF_6. In each instance BF_3 was detected by IR analysis. For a reaction in which there was a 3:1 molar excess of IrF_6 to BN, IrF_5 was observed as the primary product, whereas when equimolar amounts of BN and IrF_6 or a slight molar excess of IrF_6 were allowed to react, IrF_4, identified by its characteristic powder pattern, was the major product.

Interaction of BN with PtF_6. PtF_6 was condensed into a Teflon-FEP tube containing BN at -196°C. Allowing the reaction vessel to warm to ambient temperature a violently exothermic reaction resulted. The BN instantly became a dark gray/black color and began to fume. The black product was sprayed along the inner walls of the Teflon-FEP tube and into the Whitey valve. There was also evidence of PtF_6 attack on the Teflon-FEP tube, indicated by blackening of the tube which also became less flexible. The X-ray pattern of the black product showed metallic platinum and the IR of the gaseous products indicated only BF_3. Running the reaction at a reduced temperature with an excess of PtF_6 resulted in the partial reduction of PtF_6 to PtF_4 as detected by X-ray.

C. Results/Discussion

The original intent of these reactions of BN with metal hexafluoride species was to oxidatively intercalate BN. However, as has been clearly demonstrated, OsF_6, IrF_6 and PtF_6 are far too potent fluorinating agents. It is possible that in initial stages (as seen in the blue coloration of the BN in the beginning of the reaction with OsF_6) some intercalation occurred, but the destructive oxidation of the BN quickly occurred in all cases. As a consequence of the heteronuclear character of BN the boron atoms are slightly positively charged (+ 0.3 e) and the nitrogen atoms are negatively charged (- 0.3 e)[16]. These positive centers at the B atoms are especially vulnerable to attack and decomposition by strong fluorinating agents such as OsF_6, IrF_6 and PtF_6.

After running several experiments it became evident that intercalation of BN was not thermodynamically feasible. In these reactions BN served, in effect, as a mild reducing agent for the hexafluorides. In an effort to take advantage of the role of BN as a mild reducer a number of reactions were run in which the

temperature and stoichiometry of the reactants were carefully controlled. In this manner we hoped to find an easy route to the preparation of some rather illusive lower metal fluorides. Of particular interest was OsF_4, which has not been well characterized, and until recently[47] could not be prepared cleanly in a quantitative fashion.

When BN was treated with half an equivalent of OsF_6 and the reaction was allowed to proceed at ambient temperature a strongly exothermic reaction took place with the formation of elemental osmium. The following reaction is believed to occur:

5.2) $2BN + OsF_6 \rightarrow 2BF_3 + N_2 + Os$

The Os metal and BF_3 were detected by X-ray and IR analysis respectively, whereas the nitrogen of BN was assumed to be liberated as molecular nitrogen and therefore would be invisible to infrared light. No residual BN was detected by X-ray analysis.

In subsequent experiments the molar ratio of OsF_6/BN was increased in an effort to only partially reduce the hexafluoride. In such experiments OsF_5 was seen as the principle solid product:

5.3) $BN + 3OsF_6 \rightarrow BF_3 + 1/2N_2 + 3OsF_5$

Again, BF_3 was seen by IR and the pentafluoride pattern was evident in an X-ray photograph. At no time was OsF_4 detected in the solid products.

When BN was allowed to react with IrF_6, varying the reactant ratios and temperature conditions the solid products were detected to be Ir, IrF_4 and IrF_5. When BN was in a 2:1 molar excess over IrF_6 metallic Ir was the solid product:

5.4) $2BN + IrF_6 \rightarrow 2BF_3 + N_2 + Ir$

When IrF_6 was in large excess over BN highly crystalline IrF_5 was produced:

5.5) $BN + 3IrF_6 \rightarrow BF_3 + 1/2N_2 + 3IrF_5$

And, finally, when IrF_6 was introduced to approximately an equimolar amount of BN while a low reaction temperature (-23°C) was carefully maintained the tetrafluoride was the dominant product:

5.6) $2BN + 3IrF_6 \rightarrow 2BF_3 + N_2 + 3IrF_4$

The IrF_4 product was less crystalline than the pentafluoride material. In several instances the product contained a mixture of the penta- and tetrafluorides of iridium.

Only two experiments with PtF_6 and BN were attempted. In the initial experiment metallic platinum was formed in a violently exothermic reaction. A follow-up experiment in which the relative amount of PtF_6 was increased also occurred in an exothermic fashion yielding a very poorly crystalline PtF_4. The balanced equations parallel those previously given for production of the metal and the tetrafluoride.

D. **Summary**

No evidence of a new BN intercalation compound was seen with OsF_6, IrF_6, or PtF_6. Instead, the BN functioned as a reducing agent in the presence of the hexafluorides. In all cases, the BN was rapidly oxidized to BF_3 and N_2 and the metal hexafluoride was correspondingly reduced to a lower metal fluoride and/or the metal. The extent of reduction of the hexafluoride depended upon several factors: (1) the stoichiometry of the reacting species, and (2) the reaction temperature. An excess of BN resulted in complete reduction of the hexafluoride to the metal, while an excess of the hexafluoride yielded the penta- and/or the tetrafluoride species. Treatment of BN with the appropriate amount of IrF_6 proved to be an effective means of preparing quite pure, crystalline IrF_5. However, the tetrafluoride of osmium could not be prepared by carefully controlling the stoichiometry and reaction conditions.

CHAPTER VI

Some Properties of Dioxygenyl Fluorometallates

I. Chemistry of Dioxygenyl Salts

A. Introduction

Salts containing the dioxygenyl cation, O_2^+, have been known since the original discovery of $O_2^+PtF_6^-$ by Bartlett and Lohmann[48] in 1960 which led the way to the subsequent discovery of noble gas compounds[49]. Shortly after Bartlett's discovery, a number of other dioxygenyl salts were prepared. Young and coworkers[50] prepared $O_2^+PF_6^-$, $O_2^+AsF_6^-$, and $O_2^+SbF_6^-$ by the low temperature reaction of O_2F_2 with the respective metal pentafluorides. The arsenic and antimony salts were reported as thermally stable at ambient temperature, whereas the phosphorus salt readily decomposed. A few months later Solomon and coworkers[51] reported the preparation of the unstable $O_2^+BF_4^-$ formed by the reaction of O_2F_2 with BF_3. In 1968 Shamir et al.[52] developed a novel route to the synthesis of $O_2^+AsF_6^-$ and $O_2^+SbF_6^-$ by photolyzing a mixture of O_2/F_2 with the appropriate metal pentafluoride. Later in that year Beal, Pupp, et al.[53] demonstrated the high pressure synthesis of $O_2^+AsF_6^-$ and $O_2^+SbF_6^-$ starting with O_2, F_2 and MF_5. In 1972 Bartlett and Leary[54] reported the synthesis of $O_2^+AuF_6^-$. In 1973 Bartlett and McKee[55] described the convenient laboratory preparation of $O_2^+Sb_2F_{11}^-$ and its controlled vacuum decomposition to give $O_2^+SbF_6^-$, and clarified the fluoroantimonate system by presenting X-ray powder data for $O_2^+SbF_6^-$ and $O_2^+Sb_2F_{11}^-$.

Edwards, Griffiths and coworkers[56-59] later reported the preparation of several new $O_2^+MF_6^-$ salts (M = Rh, Ru, Bi, Nb, and Pd) and some $O_2^+M_2F_{11}^-$ salts (M =

Bi, Nb, and Ta). Subsequently, Brown et al.[60] claim to have prepared $O_2^+CrF_4Sb_2F_{11}^-$ by initially making $CrF_4Sb_2F_{11}$ from the reaction of CrF_5 with SbF_5 then exposing it to molecular O_2. In 1975 Christe et al.[61] describe the preparation of the dioxygenyl salt, $O_2^+GeF_5^-$, which is thermally unstable below room temperature.

The O_2^+ salts are very strong one-electron oxidizers as evidenced by the high electron affinity[62] of the free ion O_2^+ (12.2 eV). The kinetic stability of the anions of $O_2^+AsF_6^-$ and $O_2^+AsF_6^-$ and their convenient preparation makes them good candidates to serve as one-electron oxidizers in the production of novel high oxidation state species. A major obstacle in exploiting these powerful oxidizers has been to find a suitable solvent. In this research it has been shown that thoroughly dried HF is an effective solvent for $O_2^+SbF_6^-$. Using anhydrous HF as the solvent the synthesis of several novel high oxidation state radical species was attempted according to the following general scheme.

6.1) $$O_2^+MF_6^- + AX \rightarrow X\cdot + AMF_6 + O_2(g)$$

The halide salts used in this research were $KClO_4$, $KMnO_4$, and $KHSO_4$ in an attempt to prepare the corresponding radical species.

B. **Experimental/Results**

Preparation of $O_2^+Sb_2F_{11}^-$ and $O_2^+SbF_6^-$. The dioxygenyl fluoroantimonate salts were prepared by heating SbF_5 with an excess of a 2:1 gaseous mixture of O_2/F_2 in a modification of the preparation first described by Beal, Pupp, et al.[53] Beal and Pupp exposed the SbF_5 to ≈ 200 atmospheres of O_2/F_2 for 1 week; however, it was found in the present research that exposure to only 10 atm total pressure of O_2/F_2 for 12 hours was sufficient to produce the salt in high yield.

The net reaction is:

$$2SbF_5 + O_2 + 1/2F_2 \xrightarrow[24\ hrs]{150\text{-}200^\circ C} O_2^+Sb_2F_{11}^- \qquad 6.2)$$

Generally, ≈ 10 grams of freshly distilled SbF_5 was placed in a Monel can fitted via a Teflon o-ring to a removable water-cooled lid. Dry O_2 and F_2 were condensed into the can in the ratio of approximately 2:1 such that the total pressure at room temperature would be ≈ 10 atmospheres. The assembly was placed in a sand bath and allowed to react overnight at 150 - 200°C. A large drop in total pressure was usually noticed after several hours of reaction. If necessary additional O_2 and F_2 were condensed into the can to permit complete reaction. Yields of 80 - 90% of colorless $O_2^+Sb_2F_{11}^-$ were typically obtained. If the reaction temperature was allowed to rise much above 250°C the product was a faint yellow-green color due to NiF_2 contamination. $O_2^+SbF_6^-$ was subsequently prepared by the vacuum decomposition of $O_2^+Sb_2F_{11}^-$ as described by Bartlett and McKee[46]:

$$O_2^+Sb_2F_{11}^- \xrightarrow{120\text{-}140^\circ C} O_2^+SbF_6^- + SbF_5 \qquad 6.3)$$

Careful monitoring of the product by gravimetry was necessary due to the small dissociation pressure of $O_2^+SbF_6^-$ at elevated temperatures.

New High Temperature Structural Phase for $O_2^+SbF_6^-$. When $O_2^+SbF_6^-$ is prepared[46] by the vacuum decomposition of $O_2^+Sb_2F_{11}^-$ at ≈ 100 - 150°C a highly crystalline cubic material is obtained (a_o = 10.13 Å) which is isomorphous with $O_2^+PtF_6^-$. All observed reflections obey the condition, $h + k + l = 2n$ and the space group is Ia3, having Z = 8 with a formula unit volume of 129.9 Å^3.

In a recent preparation SbF_5 was treated with a large excess of O_2 and F_2 at a slightly higher temperature than usual (≈ 280°C). The X-ray powder pattern of the bulk product was indexed on the basis of a NaCl-type unit cell with a_o = 8.14 Å. With Z = 4 the volume per formula unit was calculated to be 134.6 $Å^3$. Another X-ray pattern was taken of some of the product which had sublimed onto the water-cooled lid. This pattern could be indexed as the usual cubic phase with a_o = 10.13 Å. The new NaCl-type phase was interpreted as a high temperature structural modification of $O_2^+SbF_6^-$. The calculated densities for the "low" and "high" temperature phases are 3.42 and 3.30 gm/cc respectively, which is consistent with what might be anticipated.

Solubility. $O_2^+SbF_6^-$ was found to be quite soluble in anhydrous HF. The HF was dried by storing over ≈ 300 - 400 mg of $O_2^+Sb_2F_{11}^-$ prior to use. 110 mg of $O_2^+SbF_6^-$ was placed in a Teflon-FEP tube and ≈ 2 ml of thoroughly dried HF was condensed onto the salt giving a 0.2 M colorless solution within a few minutes with no detectable gas evolution. Gas evolution was observed only when the HF was distilled directly from the cylinder onto an O_2^+ salt without prior treatment. Over 95% of the $O_2^+SbF_6^-$ could be recovered after 30 minutes dissolution in AHF (A: anhydrous). The X-ray powder pattern of the recovered salt showed crystalline $O_2^+SbF_6^-$. A Raman spectrum of the freshly recovered salt showed bands at 290 cm^{-1}, 589 cm^{-1} and 656 cm^{-1} which could be assigned to the ν_5, ν_2 and ν_1 bands of SbF_6^-, and a sharp band at 1861 cm^{-1} attributed to O_2^+ [55]. A solution Raman in a 1/4" Teflon-FEP tube was attempted but the instrument signal was too weak to give any meaningful results.

$O_2^+Sb_2F_{11}^-$ didn't dissolve as cleanly in AHF as did $O_2^+SbF_6^-$. On several occasions $O_2^+Sb_2F_{11}^-$ was dissolved in AHF to the extent of ≈ 0.1 M yielding a

colorless solution with no gas evolution evident. About 1 hr of dynamic evacuation of the HF was necessary to give a friable, colorless powder which typically weighed 80 - 85% of the starting material. The powder pattern of this material generally showed a weak cubic $O_2^+SbF_6^-$ pattern with some additional weak lines which could be attributed to the stronger lines of $O_2^+Sb_2F_{11}^-$. It is possible that upon evacuation of the AHF some SbF_5 was lost, leaving behind $O_2^+SbF_6^-$, which, because of its highly crystalline nature might swamp-out the less crystalline $O_2^+Sb_2F_{11}^-$ in the X-ray powder pattern. This would also account for the low recovery of the starting material. On a separate occasion dissolution and recrystallization of the $O_2^+Sb_2F_{11}^-$ gave a colorless powder which had a unique X-ray powder pattern. The pattern appeared to be of a material with a slight distortion from cubic symmetry. Attempts to index the pattern were unsuccessful. It is possible that HF may have been incorporated into the solid,

6.4) $O_2^+Sb_2F_{11}^- + 2HF \rightarrow O_2^+H_2F^+(SbF_6^-)_2$

or, perhaps the pattern represented a low temperature structural form of $O_2^+Sb_2F_{11}^-$. The gravimetry of the product showed that there was no significant weight increase which would have accompanied the reaction given in eqn. 6.4. This material was never reproduced.

Reaction of $O_2^+AsF_6^-$ with KF in AHF. $O_2^+AsF_6^-$ was dissolved in HF ($\approx$ 0.02 M) giving a colorless solution, which remained colorless even upon slight warming (50°C). These observations support the dissolution of the salt as ionic species (eq. 6.5) rather than solvated neutrals (eq. 6.6):

$$6.5) \quad O_2^+AsF_6^- \xrightarrow{HF} O_2^+(HF)_x + AsF_6^-(HF)_y$$

HF

6.6) $O_2^+SbF_6^- \rightarrow O_2F\cdot + AsF_5$

To this colorless solution approximately 2 equivalents of KF were added via a side-arm joined to the main assembly by a Teflon T connector. All of the KF dissolved resulting in a yellow-orange coloring of the solution which persisted for several minutes before vanishing. There was a small amount of gas evolution likely due to the dissociation of O_2F. These observations are best explained by the following sequence of reactions:

6.7) $O_2^+(HF)_x + AsF_6^-(HF)_{x'} + KF \rightarrow KAsF_6 + O_2F\cdot$ (red?)

6.8) $O_2F\cdot \rightarrow O_2(g) + 1/2\ F_2(g)$

The volatile gases were expanded into an IR cell immediately after the addition of HF which showed only a strong HF spectrum. The X-ray powder pattern showed a mixture of KF and $KAsF_6$.

Reaction of $O_2^+Sb_2F_{11}^-$ with KF. Equimolar quantities of $O_2^+Sb_2F_{11}^-$ and KF were loaded into a Teflon-FEP tube in the Dri-lab and fitted with a Whitey valve. Pretreated HF was condensed into the reactor resulting in a colorless solution within a few minutes with no gas evolution. The AHF was evacuated and an X-ray pattern was taken of the colorless solid which showed two cubic patterns having a_o values of 10.14 Å and 10.19 Å, corresponding to $O_2^+SbF_6^-$ and $KSbF_6$ respectively:

HF

6.9) $O_2^+Sb_2F_{11}^- + KF \rightarrow O_2^+SbF_6^- + KSbF_6$

This reaction provides a method for the quantitative production of $O_2^+SbF_6^-$ (in combination with the inert $KSbF_6$), hence avoiding the rather time-consuming vacuum thermal decomposition of $O_2^+Sb_2F_{11}^-$.

Reaction of $O_2^+Sb_2F_{11}^-$ with 2KF. $O_2^+Sb_2F_{11}^-$ and KF were placed into a Teflon-FEP tube in the Dri-lab in the molar ratio of 1:2. The reactor was removed from the Dri-lab and AHF was condensed in. Within 5 minutes a colorless solution was obtained accompanied by a small amount of gas evolution. The reaction is believed to proceed as follows:

$$6.10) \quad O_2^+Sb_2F_{11}^- + 2KF \xrightarrow{HF} 2KSbF_6 + O_2F\cdot \Downarrow O_2(g) + 1/2\ F_2(g)$$

AHF was removed by several hours of evacuation leaving a colorless friable solid. Powder diffraction of the product showed a single cubic phase with a_o = 10.19 Å corresponding to $KSbF_6$. An IR of the evolved gases showed only HF with no indication of O_2F.

Attempted Syntheses of New O_2^+ salts:

$O_2^+(HF)_x^-$. Previous observations support the dissolution of $O_2^+MF_6^-$ (M = As, Sb) in AHF as solvated O_2^+ and MF_6^- ions rather than as the neutral species $O_2F\cdot$ and MF_5. Hence, the following reaction does not occur to a significant extent at room temperature:

$$6.11) \quad O_2^+ + F(HF)_x^- \rightarrow O_2F + xHF$$

O_2F is a better base than the hydrofluoride ion, $F(HF)_x^-$ ($1 \leq x \leq 4$). This suggest the possibility of preparing a dioxygenyl salt of the hydrofluoride ion, $O_2^+F(HF)_x^-$, by the reaction of O_2F with HF according to the following general scheme:

$$6.12) \quad O_2F\cdot + xHF \rightarrow O_2^+F(HF)_x^-$$

In the present research an experiment was run in an attempt to prepare such a dioxygenyl salt. Approximately 5 ml of AHF was condensed into a 12" length of 1/2" o.d. Teflon-FEP tubing fitted with a Whitey valve. 625 torr (≈ 1 mmol) each of O_2 and F_2 were admitted into the reactor at -78°C and allowed to warm to room temperature with no indication of reaction. The Teflon-FEP tube was submerged into a -78°C slush bath contained in an unsilvered dewer. The mixture was irradiated by means of a low pressure Hg UV lamp positioned just outside of the dewer, and the entire assembly was wrapped with aluminum foil paper. After 1 hour of irradiation the HF solution became an orange color with no evidence of precipitation. When the reactor was removed from the low temperature bath the orange color disappeared within 20-30 seconds. The compound responsible for the orange color may have been O_2F_2 which is known to decompose above -57°C to molecular oxygen and fluorine:

$$\text{6.13)} \quad O_2F\cdot + F\cdot \xrightarrow{T > -57^\circ C} O_2F_2 \rightarrow O_2 + 1/2F_2$$

The mixture was again placed in the temperature bath and irradiated for an additional 2 hours. The resulting solution was a faint orange color. The HF was slowly evacuated at -78°C over a 5 hour period, leaving no solid residue.

<u>$AsF_5/S_2O_6F_2/O_2$.</u> As mentioned earlier, the dimeric peroxide, $S_2O_6F_2$, is in equilibrium with the monomeric radical, $SO_3F\cdot$:

$$\text{6.14)} \quad S_2O_6F_2 \rightleftarrows 2SO_3F\cdot$$

The free radical is a cherry red color which can be readily seen by heating $S_2O_6F_2$ in a glass tube. Also when $Xe(SO_3F)_2$ is prepared by the following reaction[22,23]:

$$\text{6.15)} \quad XeF_2 + 2HSO_3F \xrightarrow{T < 0^\circ C} Xe(SO_3F)_2 + 2HF$$

a bright red color is seen to grow in as the reaction vessel is allowed to warm from -78 to 0°C. This red color is attributed to the fluorosulfate radical. When AsF_5 is added to $S_2O_6F_2$ the following equilibrium is established:

6.16) $AsF_5 + 1/2S_2O_6F_2 \rightleftarrows AsF_5SO_3F\cdot$

The resulting radical species would likely have a considerable electron affinity and may be able to oxidize molecular oxygen:

(?)

6.17) $AsF_5 + 1/2S_2O_6F_2 + O_2 \rightarrow O_2^+(AsF_5SO_3F)^-$

Aubke and coworkers[63] have prepared $ClO_2^+(AsF_5SO_3F)^-$ from the reaction of AsF_5 with $ClO_2^+SO_3F^-$. Several experiments were run in an attempt to prepare the above dioxygenyl salt.

Approximately 5 mmols of AsF_5 (0.85 gms) and 2.5 mmols of $S_2O_6F_2$ (0.5 gms) were tensimetrically condensed into a flame-dried 100-ml quartz vial fitted with a Whitey valve. The liquids formed a faint yellow miscible solution with a room temperature vapor pressure of 1120 torr. Approximately 2 atmospheres of O_2 (8 mmol) was admitted to the reaction vessel. The mixture was vigorously stirred for 2 hours with no indication of a reaction. The liquid was slowly evacuated at 0°C leaving no solid residue.

In a second experiment 18.0 mmols of AsF_5 and 9.0 mmols of $S_2O_6F_2$ were condensed into a pre-passivated 245 ml Monel can fitted with a removable water-cooled lid. An excess of O_2 was condensed in at -196°C such that the room temperature O_2 pressure would be ≈ 14 atmospheres (125 mmols). The can was warmed to 180°C in a sand bath and the reaction was allowed to proceed overnight. Subsequently, the reaction vessel was cooled to -23°C and the volatile gases were evacuated. The can was transferred into the Dri-lab where 0.4 gm of a white/faint yellow friable powder was recovered. Exposing

this powder to water results in a mildly exothermic reaction, quite different from the strongly exothermic reaction that occurs when a dioxygenyl salt is exposed to water. The X-ray data of the product shows a fcc-type pattern, with a = 12.1 Å which may be due to a complex arsenic oxide species.

Reaction of $O_2^+SbF_6^-$ with $KClO_4$. $KClO_4$ was dried by evacuation at 150°C overnight. A 50% molar excess of $O_2^+SbF_6^-$ was added to $KClO_4$ in a Teflon-FEP tube in the Dri-lab. The colorless powders were mixed with no indication of reaction. The reaction vessel was removed from the Dri-lab and AHF was condensed in at -78°C. As the mixture warmed to room temperature there was significant gas evolution with no coloring of the solution. The evolved noncondensible gas was measured tensimetrically to be ≈ 70% of that expected if all of the O_2^+ was reduced to O_2. An IR of the volatile gases at -78°C showed weak bands assignable to CF_4 while an IR of the room temperature volatiles showed only HF. The AHF was slowly evacuated leaving a colorless powder whose X-ray pattern showed only $KSbF_6$. The gravimetry supported $KSbF_6$ as being the only solid product. There was no direct evidence of the production of the perchlorate radical. It may have existed briefly, then disproportionated to lower chlorine oxides and O_2.

6.18) $$O_2^+SbF_6^- + KClO_4 \rightarrow KSbF_6 + O_2(g) + ClO_4\cdot \ (?)$$

$$\Downarrow$$

$$ClO_x + O_2$$

Reaction of $O_2^+SbF_6^-$ with $KHSO_4$. A 50 % molar excess of $O_2^+SbF_6^-$ was added to dry $KHSO_4$ contained in a Teflon-FEP tube and 5 ml of AHF was condensed in. Once again there was no noticeable coloration of the solution accompanied

by significant gas evolution corresponding to that expected for quantitative reduction of O_2^+ to O_2(g). The X-ray pattern and gravimetry confirmed that $KSbF_6$ was the only solid product.

<u>KNO_3 and $KMnO_4$.</u> It was found that the nitrate and permanganate salts of potassium decomposed in AHF. When AHF was placed on KNO_3 there was gas evolution, while $KMnO_4$ decomposed yielding a dark green solution. The following net reactions are believed to account for these observations:

6.19) $KNO_3 + 3HF \rightarrow K^+ + NO_2^+ + H_3O^+ + 3F^-$

6.20) $KMnO_4 + 3HF \rightarrow MnO_3F$ (green) $+ H_3O^+ + KF + F^-$

Engelbrecht and Grosse[64] have isolated MnO_3F from the reaction of $KMnO_4$ with HSO_3F.

C. Summary

Thoroughly dried HF is an effective solvent for the dioxygenyl system, solvating the oxygen primarily as the cationic entity O_2^+ rather than as O_2F. This suggests that a dioxygenyl hydrofluoride salt, $O_2^+F(HF)_x^-$, might be preparable under the appropriate conditions. $O_2^+Sb_2F_{11}^-$ reacts with 1 equivalent of KF to produce a 1:1 solid mixture of $O_2^+SbF_6^-$ and $KSbF_6$ and with 2 equivalents of KF to give $KSbF_6$. Therefore, O_2F, $F(HF)_x^-$, and KF can be arranged in the order of increasing fluorobasicity as follows:

$$F(HF)_x^- < O_2F < KF$$

AsF_5 and $S_2O_6F_2$ form a faint yellow miscible solution whose color is likely due to the radical species $AsF_5SO_3F\cdot$. This radical should have a large electron affinity but appears to be inadequate to oxidize molecular oxygen under rather mild conditions.

II. Reaction of Chlorine with O_2^+

B. Introduction

When Cl_2 is placed on O_2^+ salts at -78°C an intensely purple colored compound is formed. This reaction was investigated with the intent of better characterizing the resulting compound. Richardson[65] first studied this system as a possible means to prepare Cl_2^+ salts according to the general equation:

6.21) $Cl_2 + O_2^+A^- \rightarrow O_2 + Cl_2^+A^-$

It was hoped that the lower ionization potential of molecular chlorine (265 kcal mol^{-1}) relative to molecular oxygen (278 kcal mol^{-1}) would compensate for the decreased lattice energy of the resulting salt. However, Richardson reported the production of a thermally unstable deep purple paramagnetic solid with essentially no O_2 evolution. The Raman spectrum of this purple solid and its reactivity toward NO, NOF and C_6F_6 supported its formulation as a salt containing the radical cation $(O_2Cl_2)^+$ with the following structure:

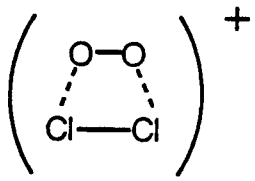

Another possibility is that the intense purple solid could contain the cationic chain polymer, $(Cl_2O_2)^+$:

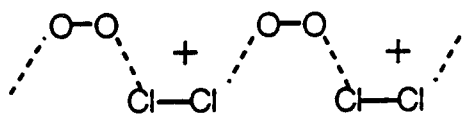

Earlier, Streng and Grosse[66] claimed to have made a "deep violet" compound, $(O_2ClF_3)_n$, by the reaction of O_2F_2 with ClF:

6.22) $O_2F_2 + ClF \rightarrow O_2ClF_3$

This compound was reported to be a strong oxidizer which was indefinitely

stable at -78°C. They obtained the same material by the interaction of O_2F_2 with Cl_2, HCl, or ClF_3. Christe[67] also reported the formation of similar violet and blue colored compounds from the reaction of $O_2^+SbF_6^-$ with ClF, ClF_3, ClF_5, ClF_3O, BrF_5, or HF; and from the reaction of $O_2^+AsF_6^-$ with $FClO_2$ or HF and $O_2^+GeF_5^-$ with HF. Christe suggested that the intensity of the violet coloration varied with the degree of dryness of HF, and could be accounted for by:

6.23) $O_2^+MF_6^- + HF + H_2O \rightarrow H_3O^+MF_6^- + O_2F\cdot$

In which the oxyfluoride radical species might be responsible for the color. ESR analysis suggested that the colored species was paramagnetic and therefore could not be explained by such diamagnetic species as O_2ClF_3. He concluded that the paramagnetic species responsible for the violet color was a polyoxygen compound, such as $(O_2)_nF$ or, possibly $(O_2)_n^+$.

B. **Experimental**

Preparation of purple compound. Typically 200 - 300 mg of $O_2^+SbF_6^-$ was placed in a Teflon-FEP tube in the Dri-lab. AHF, dried by storing over $O_2^+Sb_2F_{11}^-$, was condensed into the reaction tube at -78°C and the mixture was stirred for several minutes. An excess of Cl_2, which was similarly dried by storage over O_2^+ salt was condensed into the vessel at -78°C. Immediately, a dark purple coloring of the solution could be seen at the surface of the liquid, suggesting that the Cl_2 was interacting with dissolved $O_2^+SbF_6^-$. No O_2 evolution occurred. After further mixing a dark purple homogenous liquid was obtained, which, after close examination with a light source, appeared to be a solution rather than a solid suspension.

The purple species was indefinitely stable at -78°C. Some samples were kept for as long as 3 weeks at this temperature with no noticeable

decomposition. Allowing the purple solution to warm from -78°C to ambient temperature it became blue, then eventually a yellow solid. Removing the HF above this yellow solid resulted in its decomposition to dark brown then black pasty material.

Composition. A vacuum stable dark purple solid could be isolated by preparing the purple solution in AHF as described above, then slowly evacuating the HF at -78°C, yielding a purple powdery solid. Since no detectable amount of gaseous O_2 was evolved it was concluded that the purple solid contained all of its original oxygen and could be assigned the general formula: $[O_2(Cl_2)_x]^+SbF_6^-$. The composition of the vacuum stable solid was extensively analyzed by 3 independent methods for a number of samples. The amount of Cl_2 incorporated in the purple solid was determined by gravimetry, elemental analysis and tensimetry of the evolved Cl_2 of the decomposed product.

The chlorine content was analyzed by gravimetry by preparing the vacuum stable compound, then allowing it to warm and decompose in an air-tight reaction vessel. Once at room temperature, the weight was immediately recorded. Large $O_2^+SbF_6^-$ sample sizes (250 - 300 mg) were chosen to minimize error. The average value for "x" in $[O_2(Cl_2)_x]^+SbF_6^-$, based on 6 samples was determined to be 1.10 (17).

The elemental analysis for chlorine content was done in our laboratory by first preparing the vacuum stable salt at -78°C then allowing it to warm and decompose. The vessel was then re-cooled and NO (g) was transferred in to reduce the chlorine to chloride. H_2O was added producing HCl; then the mixture was exposed to air and titrated with standard $AgNO_3$ using chlorofluoroscein indicator. The reaction sequence is given below:

$$1/2Cl_2 + NO \rightarrow NOCl$$

$$NOCl + H_2O \rightarrow HCl + HNO_2$$

$$HCl + AgNO_3 \rightarrow AgCl + HNO_3$$

Elemental analysis on four samples showed x to be 1.14 (10).

Finally, the chlorine content was determined tensimetrically, by decomposing the vacuum stable salt at ambient temperature. Subsequently, the reaction vessel was cooled to -196°C and the noncondensible gases were removed. The remaining room temperature volatiles gas (assumed to be Cl_2) was expanded into a known volume and the pressure was recorded. Infra-red analysis of the room temperature volatiles showed no IR-active species. Three such analyses on different samples was performed giving an average value for x of 0.87 (7). The results are summarized in table 6.1.

The slightly high values for the chlorine content determined by gravimetry and elemental analysis (x = 1.10, 1.14) may be due to chlorine attack on the stainless-steel valve and fittings. This would give an artificially high chlorine analysis and gravimetry. At the same time chlorine attack on the stainless-steel vessel would cause a reduced chlorine pressure and hence a low value for the tensimetric analysis for chlorine.

X-ray. Cl_2 was slowly added to a Teflon-FEP/stainless-steel reaction vessel containing AHF over $O_2^+SbF_6^-$ producing the purple compound described earlier. The 1/4" Teflon-FEP tube had previously been drawn down to a 0.8 mm capillary for the purpose of conducting an *in situ* X-ray analysis of the product. At -78°C a vacuum stable material was prepared and a low temperature X-ray (≈ -100°C) was taken. The result was a weak cubic pattern [a_o = 10.09(3) Å] not unlike that of $O_2^+SbF_6^-$ [a_o = 10.13(1) Å]. It is possible that the purple

compound may be quite amorphous and therefore, would not diffract X-rays very strongly. The cubic pattern may be due to some residual $O_2^+SbF_6^-$ which would be very crystalline providing a strong pattern. The smaller a_o value is barely significant, but probably reflects some anticipated contraction as a consequence of F ligand libration at the lower temperature.

Decomposition products. If the vacuum stable purple solid prepared at -78°C was allowed to warm to room temperature it rapidly decomposed to a dark paste. An IR spectrum of the resulting volatiles showed only a trace of HF with no other IR-active components. Exposing the gases to a reservoir of dry Hg a milky film quickly developed characteristic of HgF_2 (or ozone), indicating that F_2 was likely evolved. The weight and viscous consistency of the solid decomposition product suggested that it was primarily SbF_5.

C. Summary

Chlorine reacts readily with $O_2^+SbF_6^-$ at -78°C in AHF producing a deep purple compound with no detectable gas evolution. Gravimetric, tensimetric, and elemental analysis studies of the -78°C vacuum stable product all indicate that 1 mole of Cl_2 is taken up per mole of $O_2^+SbF_6^-$. Richardson[65] had shown that the material is paramagnetic and has a Raman spectrum with bands at 271 cm^{-1} and 532 cm^{-1} which may be due to fundamental and first overtone of the Cl-Cl stretching mode. Therefore, the purple color is likely due to a $(O_2Cl_2)^+$ radical cation species:

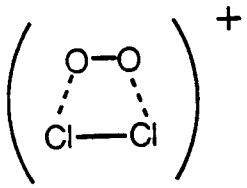

The observed high solubility of the purple compound in AHF argues against the presence of an $(O_2Cl_2)^+_n$ cationic chain polymer, but would support a monomeric entity - perhaps solvated.

Sample size (mg $O_2^+SbF_6^-$)	"x" in $[O_2(Cl_2)_x]^+SbF_6^-$ gravimetry	E. Analysis	tensimetry
262.0	0.95	1.04	-
253.1	1.16	1.25	-
226.0	1.39	1.08	-
271.3	1.09	1.18	-
267.5	1.10	-	0.93
303.6	0.93	-	0.80
299.4	1.07	-	0.89
<x> =	1.10	1.14	0.87

Table 6.1. Data obtained from the gravimetric, elemental and tensimetric analyses for the chlorine content of $[O_2(Cl_2)_x]^+SbF_6^-$.

CHAPTER VII

Silver (III) Fluoro-Complexes and Some Observations with Gold (III) Compounds

A. Introduction / Background

Sharpe[68] prepared the first $M^+AuF_4^-$ (M = Ag, Na, K) in 1949 by dissolving the appropriate metal or metal halide in BrF_3. Bromine trifluoride is a particularly effective fluorinating agent due to its ability to dissolve the metal or metal halide and the resulting product. Shortly afterward, Hoppe and Klemm[69] prepared $M^+AuF_4^-$ (M = K, Cs) by the direct fluorination of the respective alkali tetrachloroaurate (III) salts at 200 - 300°C and showed them to be diamagnetic. Peacock[70] studied potassium tetrafluoroaurate (III) and showed it to possess similar unit cell dimensions to the potassium tetrafluorobromate (III), suggesting that the AuF_4^- anions likely adopted a square planar configuration. Edwards and Jones[71] solved the structure of $KAuF_4$ by neutron diffraction demonstrating the salt to be isostructural with $KBrF_4$. The AuF_4^- anion consisted of 4 fluorine atoms disposed in a square planar array about the central Au atom. This geometry is consistent with a low spin d^8 configuration which would account for the observed diamagnetism.

Hoppe[72] prepared the first $M^+AgF_4^-$ salts (M = K, Cs) by fluorination of equimolar mixtures of $AgNO_3$ and either KCl or CsCl at 200 - 400°C. These diamagnetic ternary silver (III) salts were shown to have the $KBrF_4$-type structure with planar AgF_4^- anions[73]. Popov and Kiselyev[74] have since reported the preparation of $MAgF_4$ (M = Na, K, Rb, Cs) by the reaction of $AgF_{1.9\text{-}2.0}$, MF and XeF_2 at 220 - 250°C. A number of other AgF_4^- salts are known including $XeF_5^+AgF_4^-$ which was prepared by Zemva and coworkers[75] by the reaction of

silver difluoride, xenon hexafluoride and krypton difluoride in anhydrous HF. This yellow salt is diamagnetic and dissolves nicely in HF to give a pale yellow solution. Recently, Zemva et al.[76] prepared the lemon yellow diamagnetic salt $XeF_5^+AuF_4^-$ by the displacement of BrF_3 from AuF_3BrF_3 with XeF_6. The Au(III) salt was shown to be isostructural with its silver analogue.

The binary gold (III) fluoride has been known for some time since its original preparation from the thermal decomposition of AuF_3BrF_3 by Sharpe[68]. The compound was described as an orange powder which decomposed to Au and F_2 only upon heating above 500°C. Asprey, Jack, Kruse and Maitland[77] conducted a structural investigation of AuF_3 by analysis of powder data concluding that the trifluoride crystallized with a hexagonal unit cell, not isostructural with other known crystalline metal trifluorides. Einstein, Trotter and Bartlett[78] later performed a single crystal structural characterization of AuF_3 showing it to be hexagonal with the space-group $P6_122$-D_6^2. A magnetic susceptibility measurement showed the trifluoride to be diamagnetic with $\chi_g = -0.13 \times 10^{-6}$ c.g.s. units.

A higher oxidation state of an element is usually more stable as a complex fluoro-anion than as a neutral binary fluoride. This is the case for Ag(III) compounds of which there are many known stable compounds of complex fluoroanions, but the neutral silver trifluoride is much less stable and has only been reported recently. Bougon and coworkers[79,80] have reported the preparation of a "red brown" AgF_3 by the oxidative fluorination of AgF_2 with KrF_2 in anhydrous HF. The magnetic moment of his red brown material was determined from three sets of measurements to be 1.15(0.5) B.M. The high paramagnetism of Bougon's AgF_3 was interpreted in terms of the mixed valency compound $Ag^{2+}(AgF_6)^{2-}$ which would have a spin-only moment of 1.73 B.M. Recently,

Zemva and coworkers[47] have prepared a "bright red" AgF_3 by its displacement from $XeF_5^+AgF_4^-$ with the Lewis acid AsF_5 or PF_5, which yielded a magnetic moment of 0.80 B.M. for the former preparation and 0.38 B.M. for the latter. The paramagnetism has been attributed to impurities. The X-ray powder data for Zemva's AgF_3 is very different than the powder data obtained by Bougon for his material, and in fact has recently been indexed[47] based on an AuF_3-type structure having a hexagonal unit cell: a_o = 5.088(10); c_o = 15.43(3) Å; V = 346 Å^3; Z = 6. Zemva observed that the bright red AgF_3 will transform to a brown solid in AHF at 20°C within a few hours giving a powder pattern essentially identical to the pattern of Bougon's material[79,80].

B. Experimental Observations

Starting materials. AgF was generally used as supplied by Ozark-Mahoning (Tulsa, OK) without further purification. For several investigations AgF was prepared in this laboratory by treating either Ag_2O or AgO with anhydrous HF. The "AgF_2" supplied by Ozark-Mahoning was shown to be slightly fluorine deficient by its X-ray powder pattern[82]. Treating this stock AgF_2 with ≈ 10 atmospheres F_2 in HF at room temperature overnight provided a more stoichiometric material. Arsenic pentafluoride (Ozark-Mahoning) was shown to be pure by IR spectroscopy. $O_2^+AsF_6^-$ and $O_2^+SbF_6^-$ were prepared as described in Chapter VI. The hydrogen fluoride was thoroughly dried by storing over $O_2^+Sb_2F_{11}^-$ prior to its use.

1. Silver Chemistry

Reaction of AgF_2 with AsF_5 in HF. AgF_2 was loaded into a Teflon-FEP tube in the Dri-lab and fitted with either a Kel-F or Teflon valve. Dry HF was condensed onto the AgF_2 producing a colorless liquid with the insoluble AgF_2 resting at the base of the tube. Upon condensing in AsF_5 at -78°C a white solid film could be seen at the liquid surface, or occasionally above the surface of the brown AgF_2 which quickly dissolved upon warming. This solid may be due to the following set of equilibria[83]:

7.1) $2HF + AgF_2 \rightleftarrows H_2F^+AsF_6^-$

7.2) $H_2F^+AsF_6^- + AsF_5 \rightleftarrows H_2F^+As_2F_{11}^-$

A high local concentration of AsF_5 in HF could precipitate the salt of the dimeric anion at low temperature. Allowing the mixture to warm to ambient temperature, while stirring vigorously, a blue coloration of the solution could be seen to grow

in. If treated with an excess of AsF_5 within about 5 minutes all of the AgF_2 was consumed with no detectable gas evolution leaving behind a white solid and a deep blue solution, similar in color to aqueous $CuSO_4$. Slow removal of the AHF by evacuation gave a light blue friable powder shown by X-ray analysis to be a mixture of $AgAsF_6$ and another pattern which will subsequently be referred to as phase A (see table 7.1). The white solid was only slightly soluble in the HF whereas the blue material was very soluble even at reduced temperature (-78°C). Exploiting these solubility differences the colorless solid was isolated by successive decantation of the HF solution and shown by X-ray analysis to be $AgAsF_6$. The mass balance in table 7.4 indicated that the colorless material, formulated as $AgAsF_6$, accounted for 1/2 of the original silver present in the AgF_2[84]. This observation suggests that the remaining silver species responsible for the blue color would be a Ag (III) complex, accounting for the oxidized disproportion product.

Reaction of AgF_2 with AsF_5 and F_2 in HF. Distilling an excess of AsF_5 onto AgF_2/HF a blue solution and white solid was obtained. In an attempt to oxidize the white solid, identified as $AgAsF_6$, F_2 (2 atm) was placed over the mixture, with vigorous stirring. Two hours reaction time at ambient temperature was generally sufficient to oxidize all of the white solid producing a more intensely colored blue solution. This is not surprising in view of the ease with which AgF is oxidized to a composition approaching AgF_2 by exposure to F_2 in anhydrous HF solution[85].

The magnetic susceptibility of the blue solution prepared as described was measured using the Faraday method in a Teflon-FEP reaction vessel. The reaction tube was attached via a T connector to a Teflon-FEP side-arm which

had been drawn down to a 5 cm length of 0.4 cm (o.d.) tubing for an in situ measurement. The concentrated solution was decanted into the side-arm and shown to be diamagnetic (χ_g = -1.1 x 10^{-6} c.g.s. units). See table 7.4 for the weights, molarity and gram susceptibility.

The blue solution could be concentrated to the extent of > 2 M (based on the known silver content). Further removal of HF yielded a dark blue paste. If subjected to a good dynamic vacuum the blue material usually became colorless over a period of 6-12 hours. On a couple of occasions the material lost its color after only 30 minutes of evacuation, and in another instance the product remained blue after 3 days of evacuation. These inconsistent observations suggested that the conversion from the blue solid to the colorless $AgAsF_6$ may have involved a catalytic decomposition reaction. X-ray analysis run on the blue material, prepared by a brief evacuation (15 - 30 min) just long enough to produce a friable blue solid, showed a powder pattern identical to phase A. Gravimetric analyses done on several samples of the blue material prepared as described correspond to $AgF_{\approx 2.5} \cdot AsF_5$. Magnetic susceptibility measurements on two different samples showed the material to be slightly paramagnetic: $\mu_{eff}(1)$ = 0.91 B.M. ; $\mu_{eff}(2)$ = 1.06 B.M. However, susceptibility measurements on similarly prepared samples by Zemva and coworkers gave magnetic moments as high as 1.58 B.M. closely approaching the spin-only value of 1.73 B.M. expected for a d^9 electron configuration.

The colorless solid obtained by further evacuation of the blue product is diamagnetic with the dominant pattern in the X-ray photograph due to $AgAsF_6$. There was also a weaker pattern which has been seen before in the preparation of $AgAsF_6$ by the reaction of AgF with AsF_5 in AHF[86]. This weaker pattern is likely due to a solvated species such as $AgAsF_6 \cdot nHF$. This is not surprising in

view of the existence of the hydrogen fluoride solvate of AgF·HF which will be discussed later in this chapter. The weight of the colorless solid corresponds to "$AgF_{\approx 1.5}$·AsF_5", or approximately midway between $AgAsF_6$ and $AgF^+AsF_6^-$, which would be consistent with half a mole of HF being incorporated into $AgAsF_6$.

Reversibility with respect to F_2. A mixture of AgF_2/AsF_5/HF produces a white solid / blue solution mixture. Treatment of this system with excess F_2 resulted in the oxidation of the colorless solid to the solvated blue species. If the HF was removed by evacuation producing a friable blue solid, then redistilled back onto the sample a white solid / blue solution mixture was again obtained. Addition of F_2 was necessary to re-oxidize the colorless material to completely dissolve it. This cycle has been repeated 3 or 4 times, each time requiring molecular fluorine to re-establish the blue solution.

If the blue solid is further evacuated to the colorless solid, and HF is redistilled back onto the material, a white solid / colorless solution is obtained. Exposure to 2 atmospheres of F_2 for several hours eventually re-oxidized the material back into solution producing the soluble blue entity. On several occasions a small amount of AsF_5 was required after exposure to F_2 to regain complete solution.

An attempt was made to obtain a blue solid which was not fluorine deficient with respect to the blue solvated species, such that the HF could be removed by evacuation producing a friable blue product, representative of the solvated entity, and which would redissolve completely in the HF. The vapor pressure of neat HF at -78°C is large enough to permit its transfer by distillation, however, when the HF contains a concentrated solution of the blue fluoro-complex the

vapor pressure is reduced to the extent that HF cannot be evacuated much below -23°C. The blue solution was prepared by $AgF_2/AsF_5/F_2/HF$ as before, and the HF was slowly removed at O°C producing a friable blue solid. Addition of HF yielded a blue solution / white solid mixture which required additional F_2 to re-establish solution. A similar experiment at -23°C required a 36 hour evacuation time to remove all of the HF giving a blue solid which again proved to be fluorine deficient relative to the totally dissolved blue silver species.

Determination of the amount of fluorine lost by evacuation of the blue solution. It was observed that when the solvated blue silver fluoro-complex was subjected to a dynamic vacuum it formed a blue solid, then eventually a colorless solid, the latter of which was shown by X-ray analysis to be $AgAsF_6$. Furthermore, the $AgAsF_6$ produced could be re-oxidized by fluorination back to the original blue solvated species. Several attempts were made to quantitate the amount of fluorine lost during the process of evacuation to characterize better the nature of the blue solvated silver fluoro-complex.

In one investigation the deep blue solution was prepared by the interaction of $AgF_2/AsF_5/F_2/HF$ as usual. Then the solution was concentrated to about 1 mmol in 0.5 ml, or about 2 M (assuming the solvated species was a monosilver complex). The Teflon-FEP apparatus containing the concentrated blue solution was attached to a double Teflon U-trap fitted with two Teflon valves. An excess of dry, finely powdered NaF was contained in the first trap to collect the HF, and in an excess of similarly prepared KI was placed in the second trap to reduce the evolved fluorine. The concentrated blue solution was subjected to a dynamic vacuum via the double U-trap. After 18 hours of evacuation the product had lost most of its color, and after 50 hours the material was completely colorless. An

X-ray powder pattern of this colorless material showed $AgAsF_6$. A brown color due to iodine production could be seen to gradually grow in the second trap, which was held at -78°C throughout the two day evacuation to avoid loss of the volatile iodine.

The KI / I_2 mixture was transferred to a flask and dissolved in distilled water. An iodometric titration was performed on the solution using standardized thiosulfate with starch indicator. The titration revealed that the solution contained 0.81 moles of I_2 [I_3^- (aq)] per mole of AgF_2 initially present, which would correspond to 0.81 moles of evolved F_2 per mole AgF_2. However, a concern in this evaluation is that the AsF_5, which was in 50% excess over AgF_2, may not have been completely complexed by the NaF and, therefore, may have accounted for some of the I_2 production, resulting in an artificially high analysis for evolved fluorine.

A second experiment was tried in which the blue complex was evacuated through successive traps containing NaF, CsF, and finally KI. The CsF, present in excess, would certainly neutralize any AsF_5 that escaped through the NaF. However, a 5 day evacuation failed to produce a colorless product. The vacuum in this system containing a series of traps may not have been sufficient to completely convert the blue compound to $AgAsF_6$. Alternatively, as mentioned earlier, the conversion from the blue solid to $AgAsF_6$ could involve a catalytic decomposition.

Reaction of $O_2^+AsF_6^-$ with AgF_2 in HF. AgF_2 was combined with a 10% molar excess of $O_2^+AsF_6^-$ in a Teflon-FEP tube and fitted with a Kel-F valve in the Dri-lab. HF was condensed onto the solid mixture. There was a small amount of gas evolution which when exposed to a reservoir of Hg formed a thin milky

surface layer characteristic of HgF_2. The reaction mixture was a familiar blue solution over a white solid. The blue solution was decanted at 0°C then concentrated by evacuation of the HF. The solution became a very intense blue color which upon removal of the last few drops of HF lost its color giving a faint pink/white solid. The X-ray pattern of this solid showed a NaCl-type cubic pattern with an a_o value of 7.90 Å. The corresponding molecular volume would be 123 $Å^3$ approximately midway between the molecular volumes for $AgAsF_6$[87] (115.9 $Å^3$) and $O_2^+AsF_6^-$ [88] (130.9 $Å^3$) supporting the possible formation of a solid solution such as $[Ag_x(1-x)O_2]^+AsF_6^-$. The small observed difference in the relative intensities of the diffracted lines between $AgAsF_6$ and the cubic phase with a_o = 7.90 Å would be expected for such a solid solution.

Reaction of $O_2^+SbF_6^-$ with AgF_2 in HF. This reaction was originally run in an attempt to prepare a Ag (III) fluoro-complex directly by exploiting the oxidizing power of O_2^+. Equimolar quantities of AgF_2 and $O_2^+SbF_6^-$ were mixed together and AHF was condensed on at -78°C. Upon warming with vigorous stirring the solution began to slowly evolve gas over a 5 minute period and gradually became an intense blue color. The noncondensible gases (at -196°C) reacted with dry Hg producing HgF_2 suggesting that there was some decomposition of the $O_2^+SbF_6^-$ to O_2F (O_2 and 1/2 F_2). At ambient temperature all of the material was in solution, but upon cooling to -78°C a white crystalline compound precipitated likely due to $AgSbF_6$ formation. The HF was evacuated yielding a powdery blue-green solid which had a quite complicated X-ray pattern containing at least 3 phases: two cubic phases identified as $O_2^+SbF_6^-$ and $AgSbF_6$, and 11 very weak lines which could not be identified nor indexed. A small amount of residual $O_2^+SbF_6^-$ would give a strong pattern due to its highly crystalline nature.

The $AgAsF_6$ appears to be the reduction product of the disproportionation of AgF_2. The corresponding oxidation product likely responsible for the blue-green color was not identified but may have given rise to the weak unidentified pattern in the X-ray.

Preparation of AgF·HF. AgF is unique among the Ag(I) halides in having a high solubility in aqueous solutions. It also is anomalous in its ability to form hydrates, $AgF{\cdot}nH_2O$ (n = 1,2)[89]. Therefore, it is not surprising that the hydrogen fluoride solvates exist. Guntz and Guntz [90]first identified the solvates AgF·nHF (n = 2/3, 1, 2, 3, 5), however no structural evidence had been obtained.

Analytically pure AgF is an orange-yellow color. It was noticed on several occasions that when AgF was prepared by the reaction of either Ag_2O or AgO with HF a colorless solid initially precipitated that had a gravimetric analysis consistent with its formulation as $AgF{\cdot}HF$[91]. An X-ray powder pattern of the colorless solid has been obtained in a 0.8 mm Teflon-FEP capillary which was indexed based on a tetragonal unit cell: a_o = 5.479 Å, c_o = 6.056 Å, Z = 4 (see table 7.2). The volume per formula unit for Ag·HF is 45.45 $Å^3$ which is similar to the 47.77 $Å^3$ formula unit volume of $NaHF_2$[92].

2. Gold Chemistry

$AuF_3/AsF_5/HF$. The reaction between AuF_3 and AsF_5 was conducted in an attempt to abstract a fluoride ion from the trifluoride and produce the cationic metal fluoride salt, $AuF_2^+AsF_6^-$. AuF_3 was prepared by the pyrolysis of AuF_3BrF_3 originally described by Sharpe[68]. Approximately 0.7 mmol of AuF_3 was placed in a Teflon-FEP tube equipped with a Kel-F valve. AHF was condensed onto the AuF_3 with no significant dissolution of the trifluoride. A two-fold molar excess of

AsF_5 was condensed on the AuF_3/HF and allowed to warm with vigorous stirring with no indication of reaction. Additional AsF_5 was condensed on providing a ten-fold molar excess of the pentafluoride. After 4 hrs of reaction time with vigorous stirring there was no hint of chemical reaction.

<u>$Au/As_2O_3/BrF_3$.</u> Two equivalents of freshly precipitated metallic gold were combined with one equivalent of As_2O_3 in the first trap of a double pyrex U-trap. Bromine and BrF_3 were condensed into the trap at -196°C and allowed to slowly warm to ambient temperature. The reaction was quite mild occurring at a slow steady rate over a period of about 15 minutes. The mixture was stirred vigorously for an additional hour at room temperature to insure complete reaction. The excess BrF_3 and Br_2 were transferred by dynamic evacuation to the second trap leaving behind a light orange product. The first trap was heated to 70 - 80°C while under vacuum for one hour to remove all of the BrF_3 from the product. The trap was sealed under vacuum with a gas-oxygen flame and transferred into the Dri-lab. The gravimetry of the orange product suggested that no significant amount of arsenic could be present. The mass balance was consistent with the formulation of the product as either a binary fluoride or oxyfluoride such as AuF_4 or $AuOF_3$. The magnetic susceptibility showed the material to be diamagnetic (χ_g = -0.2 x 10^{-6} c.g.s. units) which ruled out its formulation as the tetrafluoride (d^7). The powder pattern revealed that the material was highly crystalline and had a general pattern quite similar to AuF_3 yet distinctly different in detail. Attempts to index the pattern were unsuccessful.

The same material was made in 1962 by Rao from the high temperature (500°C) flow-system fluorination of AuF_3 in a silica tube. His analysis showed

that the material contained 74.2% Au, and 20.3% F by weight which doesn't clearly distinguish between AuF_3 (Au : F :: 77.6 : 22.4) and $AuOF_3$ (Au : F : O :: 73.0 : 21.1 : 5.9). Rao also conceded in his notes that the fluorine analysis was low due to spillage.

AgF/Au/BrF_3. AgAuF4 was prepared in a manner similar to the method described by Sharpe[68] involving distilling BrF_3 onto an equimolar mixture of Ag/Au. For this preparation equimolar quantities of AgF and recently precipitated Au powder were mixed together in a flame-dried double pyrex U-trap. BrF_3 was condensed on and a rather vigorous reaction ensued. After several hours the Br_2 was removed by evacuation leaving behind a bright yellow solution. The product was very soluble in the BrF_3 as evidenced by its precipitation as a pale yellow solid only after the last of the solvent was removed. The gravimetry was in good agreement with the formulation of the product as $AgAuF_4$, and the reported diamagnetism[73] of the compound was confirmed by a susceptibility measurement. The X-ray powder pattern showed the $AgAuF_4$ to be quite crystalline possessing the $KBrF_4$-type structure common to other known $MAuF_4$ (M = Na, K, Rb) salts. The indexed powder pattern is given in table 7.3.

$AgAuF_4$ / F_2. The synthesis of $AgAuF_6$ was attempted by the high-temperature / high pressure fluorination of $AgAuF_4$. Approximately 1.1 mmol of $AgAuF_4$ was placed in a prepassivated Ni-boat contained in a Monel can with a removable water-cooled lid. Fluorine was condensed in such that its vapor pressure would be 20 atmospheres at 200°C. The can was heated to 210°C overnight, then transferred to the Dri-lab where the solid yellow product was loaded into a capillary and shown by X-ray analysis to be $AgAuF_4$. Higher temperature /

pressure conditions may be necessary to oxidize the tetrafluoride.

C. Discussion

A number of experiments indicate that when AsF_5 is placed on AgF_2 in anhydrous HF the silver (II) undergoes a disproportionation reaction to silver (I) and silver (III). When this reaction is carried out two distinct phases are immediately evident in the final product: a deep blue solution and a colorless solid. The colorless solid has been isolated by successive decantation of the more soluble blue complex and identified by X-ray analysis to be $AgAsF_6$, which has been shown by gravimetry to contain half of the silver originally present in the AgF_2[84]. Therefore, since no detectable amount of gaseous F_2 is evolved from the system, and its solubility in anhydrous HF is quite low[93], the oxidized disproportionation product must be a Ag (III) fluoro-complex to account for the charge balance. The following disproportionation reaction is proposed to account for the experimental observations:

$$7.3) \quad 2AgF_2 + 2AsF_5 \xrightarrow{HF} \underset{\text{(white)}}{AgAsF_6\,(s)} + \underset{\text{(blue)}}{AgF_2^{+}(HF)_x} + AsF_6^{-}(HF)_y$$

Associated with the disproportionation of Ag(II) to Ag(I) and Ag(III) is a change in the electron configuration from d^9 to d^{10} and d^8, respectively. Salts of the silver (III) fluoro-anion, AgF_4^-, are diamagnetic. This is consistent with a low-spin d^8 electron configuration, and analytically pure AgF_3 may well be diamagnetic low-spin d^8 since it has recently been shown to be isostructural with AuF_3[81] and therefore must involve roughly square-planar $[AgF_4]^-$ units linked by cis fluoro bridges in hexagonal spiral chains. Therefore, the silver (III) fluoro-cation, AgF_2^+, (which is presumably solvated by the HF) may also be square

coordinated Ag(III) and therefore of low-spin electron configuration. Thus the low-spin d^8 electron configuration in combination with the solvation energy of the AgF_2^+ cation may be a large factor in driving the disproportionation of the silver (II). It is of interest that AgF_2 is a genuine AgII (d^9) material but, disproportionation into Ag(I) and Ag(III) is favored in AgO which has the formulation $Ag(I)Ag(III)O_2$ and is diamagnetic[94].

Frlec, Gantar, and Holloway[95,96] have studied the reaction of excess AsF_5 with a number of MF_2 compounds (M = Fe, Cu, Zn, Cr, Ag, and Sn) in anhydrous HF. They claimed that the AsF_5 formed a 1:1 adduct with AgF_2 producing the blue compound, "$AgF_2 \cdot AsF_5$", which undergoes thermal decomposition as follows:

$$7.4) \quad AgF_2 + AsF_5 \xrightarrow{HF} AgF_2 \cdot AsF_5$$

$$7.5) \quad AgF_2 \cdot AsF_5 \xrightarrow{65\text{-}352^\circ C} 2AgF_2 \cdot AsF_5 \xrightarrow{352\text{-}600^\circ C} AgF_2 \rightarrow AgF + Ag + F_2$$

In a recent publication by Gantar et al.[97] the crystal structure of $AgF_2 \cdot AsF_5$ was reported. The compound, grown from anhydrous HF, was shown to be orthorhombic with the space group Pnma. The structure consists of an infinite F-bridged cationic chain, $(Ag\text{-}F)_n^{n+}$, with AsF_6^- octahedra cross-linked to these chains through F-bridges. Each Ag occupies a pseudo-pentagonal bipyramid environment of fluorines. The final R value was 0.032. No mention is made of a heterogenous product, yet in the present research in this laboratory, a two-phase mixture was invariably produced from the reaction between AsF_5 and AgF_2 in AHF.

The X-ray powder pattern of the product of the reaction between AgF_2 and AsF_5 in the present research shows a two phase mixture of $AgAsF_6$ and phase A. Exposure of this mixture to 2 atmospheres of F_2 for two hours at ambient

temperature produces a blue solution which upon brief evacuation gives a friable blue product with an X-ray pattern identical to phase A. Phase A can be indexed quite convincingly according to a computer generated pattern based on the unit cell of $AgF^+AsF_6^-$ determined by Gantar and coworkers[97].

The magnetic susceptibility of the blue solid, identified as $AgF_2AsF_6^-$ was measured for two samples to be 0.9 and 1.1 B.M. Similarly prepared samples by Zemva and coworkers have a measured magnetic moment as high as 1.58 B.M., approaching the spin-only value of 1.73 B.M. expected for a compound with a d^9 electron configuration. Yet, to account for the disproportionation of AgF_2 when treated with AsF_5 alone in AHF the blue solution species must be formulated as Ag(III).

The blue $AgF^+AsF_6^-$ obtained by careful removal of HF is not representative of the blue solution species since the $AgF^+AsF_6^-$ is not very soluble in HF. In addition, a magnetic susceptibility measurement of the concentrated blue solution showed it to be diamagnetic, $\chi_g = -1.1 \times 10^{-6}$ c.g.s. units, whereas $AgF^+AsF_6^-$ is paramagnetic. Diamagnetism is consistent with a low-spin d^8 configuration expected for Ag(III). Careful evacuation of the HF from the blue solution, either at ambient temperature or at -23°C, results in a blue powder which is fluorine deficient with respect to the solvated species. The concentrated blue solution can be re-established by the addition of F_2. However, it was found that when the blue solution was subjected to a dynamic vacuum at -78°C for 6 hours there was no loss in color intensity or solid precipitation. Fluorine would have readily been removed at this temperature if there were an equilibrium interaction between the solution species, AgF_2^+, AgF^+ and gaseous F_2.

The species which gives rise to the blue color, believed to be AgF_2^+, may be stable only when solvated by HF. It may well decompose upon removal of solvent:

$$7.6) \quad AgF_2^+(HF)_x + AsF_6^-(HF)_{x'} \xrightarrow{-HF} \underset{\text{blue}}{AgF^+AsF_6^-(s)} + 1/2\ F_2$$

In a series of experiments Zemva, Lutar, Jesih, Casteel and Bartlett[47] have observed that when a yellow solution of $XeF_5^+AgF_4^-$ is treated with one equivalent of AsF_5 a quantitative precipitation of the bright red AgF_3 results:

$$7.7) \quad XeF_5^+AgF_4^-(HF) + AsF_5 \xrightarrow{20°C} AgF_3(red) + XeF_5^+AsF_6^-(HF)$$

An additional equivalent of AsF_5 results in the disappearance of the red AgF_3 and the formation of a deep blue solution accompanied by a small amount of F_2 evolution[98]. The evolved fluorine was measured tensimetrically to be ≈1/6 mole F_2 per mole of AgF_3. These observations support the formation of a solvated Ag(III) fluoro-cation which may be responsible for the blue coloration.

$$7.8) \quad AgF_3 + AsF_5 \xrightarrow{HF} \underset{\text{(blue)}}{AgF_2^+(HF)_x} + AsF_6^-(HF)_{x'} + 1/6\ F_2$$

The small amount of evolved F_2 is likely associated with the heat of reaction. Zemva and his coworkers have observed that if the anhydrous HF is allowed to remain over the bright red AgF_3 it will transform into a red brown solid shown by X-ray analysis to be the material prepared by Bougon[79,80] by the reaction of KrF_2 with AgF_2.

If AsF_5 is placed on this red brown solid in HF a blue solution is again seen; however, there remains a considerable amount of brown solid at the base of the reaction tube. The brown solid is believed to be AgF_2, but this has not yet been established. These observations are consistent with the bright red AgF_3 being the stoichiometric binary trifluoride, and the red brown material being slightly fluorine deficient with respect to AgF_3.

D. **Summary**

When AgF_2 is exposed to AsF_5 in anhydrous HF it rapidly undergoes a disproportionation reaction producing a colorless solid and a blue solution. The colorless solid, identified as $AgAsF_6$ was shown by mass balance to contain one-half of the Ag originally present in AgF_2. Therefore, since no detectable amount of F_2 was evolved and its solubility in anhydrous HF is negligibly small the oxidized disproportionation product must be $AgF_2^+AsF_6^-$. Exposure of this mixture to F_2 oxidizes the Ag(I) to Ag(III) producing a homogenous concentrated blue solution (which can exceed 2 M). The magnetic susceptibility of the blue solution shows the dissolved species to be diamagnetic, in accord with the low-spin d^8 electron configuration expected for Ag(III). These conclusions are consistent with the observations of others[98] that when AgF_3 is treated with an equimolar quantity of AsF_5 an intense blue solution is formed with the evolution of ≈1/6 mole of F_2 presumably due to thermolysis of some of the AgF_3 in the hot reaction. This blue entity must be formulated as the silver (III) fluoro-complex, $AgF_2^+AsF_6^-$. The AgF_2^+ cation is stable only when solvated by HF and rapidly decomposes to AgF^+ upon removal of the solvating HF. The magnetic susceptibility of $AgF^+AsF_6^-$ approaches the spin-only value expected for a d^9 electron configuration. The $AgF^+AsF_6^-$ salt disproportionates to Ag^+ and AgF_2^+ when HF is condensed on it. This mixture can be reoxidized with F_2 back up to AgF_2^+ completing the reversible cycle:

7.9) $AgF_2^+AsF_6^-$ (solv.) ⇌ $AgF^+AsF_6^-$ (solid)

-HF, -1/2 F_2 (forward); HF, 1/2 F_2 (reverse)

Table 7.1 X-ray data for blue solid ($AgF^+AsF_6^-$). Observed $1/d^2$ values with corresponding visual intensities. Calc. $1/d^2$ generated from the unit cell of $AgF^+AsF_6^-$.[97]

	$AgF^+AsF_6^-$ from:			$AgF_2 + AsF_5 + F_2$ / HF			
I	$1/d^2$ (obs)	$1/d^2$ (calc)	hkl*	I	$1/d^2$ (obs)	$1/d^2$ (calc)	hkl*
S	0.0312	0.0307	001	MW	0.4774	0.4757	502
S	0.0488	0.0481	111	VW	0.4964	0.4957	325
W	0.0620	0.0586	102	VW	0.5120	0.5109	235
VW	0.0679			VVW	0.5431	0.5477	513
W	0.0714	0.0695	200	MW	0.5624	0.5612	244
S	0.0809	0.0798	201	MW	0.6089	0.6090	523
S	0.0833	0.0817	020	MW	0.6282	0.6287	531
VW	0.0921	0.0900	211	MW	0.6532	0.6539	245
VW	0.1056			MW	0.6603	0.6596	532
MS	0.1149	0.1131	013	VW	0.7023	0.6977	046
VW	0.1249	0.1229	022	M	0.7261	0.7307	426
MS	0.1336	0.1305	113	M	0.7564	0.7598	353
MW	0.1437	0.1403	122	W	0.7793	0.7765	062
MW	0.1657	0.1649	004	M	0.8062	0.8059	506
VVW	0.1703	0.1667	301	MW	0.8186	0.8199	631
VW	0.1859	0.1827	213	MW	0.9084	0.9037	605
VVW	0.1918	0.1918	123	MW	0.9172	0.9175	164
W	0.1971	0.1976	302	M	1.0211	1.0237	461
VW	0.2223	0.2181	312	MW	1.0531	1.0546	462
MW	0.2496	0.2492	303	VW	1.0983		
MW	0.2590	0.2548	214	MW	1.1178	1.1176	644
W	0.2687	0.2696	313	MW	1.1849	1.1805	636
MS	0.2817	0.2793	322	W	1.2184	1.2197	742
MW	0.2994	0.2985	411	MW	1.2369	1.2353	822
MW	0.3142	0.3161	224	W	1.3144	1.3144	637
MW	0.3250	0.3268	040	W	1.3166	1.3161	556
MW	0.3327	0.3309	323	W	1.3029	1.3012	654
VW	0.3453	0.3461	233	MW	1.3902	1.3904	815
VW	0.3515	0.3506	331	MW	1.3972	1.3966	367
VW	0.3659	0.3661	134	W	1.4691	1.4689	638
VW	0.3752	0.3709	006	W	1.4935		
VW	0.3969	0.3963	240	W	1.5102	1.5111	708
MW	0.4068	0.4066	240	VW	1.5175	1.5183	467
M	0.4139	0.4040	305	VW	1.5508	1.5511	368

* conditions limiting possible reflections: hk0, h+k=2n; 0kl, k+l=2n; h00, h=2n; 0k0, k=2n; 00l, l=2n.

Table 7.2. X-ray powder data for AgF·HF obtained from reaction of Ag_2O with anhydrous HF. Data were fit using least-squares calculation.

AgF·HF: tetragonal, a_o = 5.486(5) Å, c_o = 6.057(8) Å			
Intensity	hkl	$1/d_2$(obs)	$1/d_2$(calc)
MS	110	0.0666	0.0665
MW	002	0.1091	0.1090
M	200	0.1328	0.1329
MS	112	0.1754	0.1755
MW	211	0.1928	0.1934
M	202	0.2424	0.2419
W	220	0.2675	0.2658
M	310	0.3329	0.3323
M	222	0.3744	0.3749
MW	004	0.4354	0.4362
MW	312	0.4406	0.4413
W	114	0.5027	0.5026
W	204	0.5687	0.5691
W	402	0.6394	0.6407
W	224	0.7037	0.7020

Table 7.3. X-ray powder data for $AgAuF_4$. The data were indexed based on a tetragonal unit cell: a_o= 5.787 Å, c_o= 5.392 Å. Data were fit using least-squares method.

$AgAuF_4$: tetragonal, a_o = 5.787(5) Å, c_o = 5.392(7) Å

Intensity	hkl	$1/d_2$(obs)	$1/d_2$(calc)
W	001	0.0344	0.0343
W	110	0.0599	0.0596
VS	111	0.0944	0.0939
M	200	0.1194	0.1192
W	002	0.1379	0.1372
VVW	201	0.1544	0.1535
VVW	112	0.1963	0.1969
M	220	0.2389	0.2385
MS	202	0.2574	0.2565
VVW	221	0.2746	0.2727
MS	311	0.3336	0.3324
M	113	0.3701	0.3684
M	222	0.3786	0.3757
VW	312	0.4370	0.4353
W	400	0.4771	0.4770
VVW	411	0.5385	0.5411
W	004	0.5517	0.5489
MW	420	0.5967	0.5962
M	114	0.6104	0.6085
MW	402	0.6147	0.6142
W	332	0.6711	0.6738
MW	422	0.7347	0.7334
MW	224	0.7890	0.7874
MW	511	0.8101	0.8094
MW	314	0.8465	0.8470
W	115	0.9197	0.9173
VW	440	0.9564	0.9539
VW	404	1.0290	1.0259
W	531	1.0479	1.0479
W	424	1.1450	1.1451
W	315	1.1548	1.1558
VVW	620	1.1931	1.1924
VVW	602	1.2085	1.2104
W	514	1.3238	1.3240
W	405	1.3319	1.3346
VVW	206	1.3539	1.3543
VW	335	1.3937	1.3943
VVW	226	1.4716	1.4736
VVW	444	1.5006	1.5028

Table 7.4. Gravimetric (a., b.) and magnetic susceptibility (c.) data for the Ag fluoro-complex system.

a.)

mass balance for: $AgF_2 + AsF_5 \rightarrow 1/2\ AgAsF_6$ + blue sol'n

mmol AgF_2	mmol $AgAsF_6$	mol $AgAsF_6$(s) / mol AgF_2	mol $AgAsF_6$ (cor.)* / mol AgF_2
0.795	0.336	0.42	0.52
1.259	0.558	0.44	0.54

* The $AgAsF_6$ was isolated by decanting off the HF sol'n at 0°C. The correction was based on the estimated solubility of $AgAsF_6$ (≈10 mg/ml HF) at this temperature.

b.)

gravimetry for blue solid ($AgF^+AsF_6^-$)

wt AgF_2(mg) initially	mmol AgF_2	wt blue solid prod.(mg)	x in $AgF_x \cdot AsF_5$
203.1	1.39	422.5	2.4
143.9	0.99	301.8	2.5
118.8	0.81	250.5	2.5

c.)

magnetic susceptibility†

blue solid ($AgF^+AsF_6^-$) μ (B.M.)	2M‡ blue sol'n ($AgF_2^+AsF_6^-$) χ (c.g.s. units)
0.91	-1.1×10^{-6}
1.06	

†measurements were corrected for diamagnetic contribution
‡the blue solution ($AgF_2^+AsF_6^-$) could be concentrated to the extent of 2 mmol Ag complex/ml HF solution without precipitation.

REFERENCES

1.) W. L. Jolly, *The Synthesis and Characterization of Inorganic Compounds*, Prentice-Hall, Inc., Englewood Cliffs, N. J. (1970).

2.) P. W. Selwood, *Magnetochemistry*, 2nd Ed., Interscience Publishers, New York (1957).

3.) A. I. Vogel, *Textbook of Quantitative Inorganic Analysis*, Longman, London and New York (1978).

4.) A. Balzorotti and Grandolfo, *Phys. Rev. Lett.*, **20** (1968), 9.

5.) J. W. McClure, *IBM J.* July, p. 255 (1964); M. S. Dresselhaus and J. G. Mauroides, *IBM J.* July, p. 262 (1964).

6.) R. C. Croft, *Aust. J. Chem.*, **9**, (1956) 206.

7.) W. Rudorff and E. Stumpp, *Z. Naturforsch.*, Teil B., **13**, (1958) 459.

8.) A. G. Freeman and J. P. Larkindale, *J. Chem. Soc.*, **A 7**, (1969) 1307.

9.) A. G. Freeman and J. P. Larkindale, *Inorg. Nucl. Chem. Lett.*, **5**, (1969) 937.

10.) K. Ohashi and T. Shinjo, *Bull. Inst. Chem. Res. Kyoto Univ.*, **55**, (1977) 441.

11.) H. Schafer, *Z. Anorg. U. Allgem. Chem.*, **259** (1949).

12.) C. Mugiya, N. Ohigashi, Y. Mori, and H. Inokuchi, *Bull. Chem. Soc. Jpn.*, **43**, (1970) 287.

13.) N. Bartlett, R. N. Biagioni, B. W. McQuillan, A. S. Robertson, and A. C. Thompson, *J. Chem. Soc. Chem. Comm.*, (1978) 200.

14.) R. N. Biagioni, Ph.D. Thesis, University of California, Berkeley (1980).

15.) O. Glemser and H. Haeseler, *Z. Anorg. Allg. Chem.*, **279**, (1959) 141.5

16.) D. J. Joyner and D. M. Hercules, *J. Chem. Phys.*, **72**, (1980) 1095.

17.) I. L. Spain, *Chemistry and Physics of Carbon*, P. L. Walker and P. A. Thrower, eds., Marcel Dekker Inc., New York. (1973).

18.) T. Renner, *Z. anorg. allg. Chem.*, 298, **22** (1958).

19.) M. J. Bottomly, G. J. Parry, A. R. Ubbelohde and D. A. Young, *J. Chem. Soc.*, (1963) 5674.

20.) A. R. Ubbelohde, *Prod. Roy. Soc.*, **A309** (1969), 297, and **A321** (1971), 445.

21.) J. G. Hooley, *Carbon*, **Vol. 31(3)** (1983), 181.

22.) N. Bartlett and F. O. Sladky, *J. Chem. Soc. Chem Comm.* (1968), 1046.

23.) M. Wechsberg, P. A. Bullinger, F. O. Sladky, R. Mews, and N. Bartlett, *Inorg. Chem.*, **11** (1972), 3063.

24.) A. Smalc., submitted to *Inorg. Synth.* (1988).

25.) F. B. Dudley and G. H. Cady, *J. Amer. Chem. Soc.*, **79** (1957), 513.

26.) S. M. Williamson, *Inorganic Synthesis*, **12** (1968), 147.

27.) N. Daumas and A. Hérold, *C. R. Hebd. Seances Acad. Sci., Ser. C.*, **268** (1969), 373.

28.) K. O'Sullivan, R. C. Thompson and J. Trotter, *J. Chem. Soc.*, **A** (1967), 2024.

29.) R. D. Shannon and C. T. Prewitt, *Acta. Cryst.*, **B26** (1970), 1076.

30.) S. Karunanithy, J. M. Willis and F. Aubke, *J. Fluorine Chem.*, **24** (1988), 379.

31.) K. O'Sullivan, R. C. Thompson and J. Trotter, *J. Chem. Soc.*, **A** (1970), 1814.

32.) F. Okino, Ph.D. Thesis, University of California, Berkeley (1984).

33.) C. Zeller, A. Denestein and G. M. T. Foley, *Rev. Sci. Instrum.*, **50** (1979), 602.

34.) Average specific room temp. conductivity value obtained based on 6 measurements of different SP1 samples by R. Kaner, K. Kourtakis, and S. G. Mayorga.

35.) T. Mallouk, Ph.D. Thesis, University of California, Berkeley, 1982.

36.) National Bureau of Standards 500, "Selected Values of Chemical Thermodynamical Properties", 1952.

37.) T. E. Mallouk, G. L. Rosenthal, G. Miller, R. Brusasco and N. Bartlett, *Inorg. Chem.*, **23** (1984), 3167.

38.) National Bureau of Standards (U.S.A.), Natl. Stand. Ref. Data Series NB 526 (1969).

39.) N. Bartlett, B. W. McQuillan and A. S. Robertson, *Mat. Res. Bull.*, **13** (1978), 1259.

40.) E. M. McCarron, N. Bartlett, *J. Chem. Soc., Chem. Comm.* (1980), 404.

41.) E. M. McCarron, Y. J. Grannec and N. Bartlett, *J. Chem. Soc., Chem. Comm.*, (1980), 890.

42.) G. V. Samsanov and V. M. Sleptsov, *Kinetika i Kataliz, Acad. Sci. USSR.*, Sb. Statei (1960), 129.

43.) T. Mallouk, B. L. Hawkins, M. P. Conrad, K. Zilm, G. E. Maciel and N. Bartlett, *Phil. Trans. R. Soc. Lond.*, A **314**, (1985) 179.

44.) S. Karunanithy and F. Aubke, *J. Fluorine Chem.*, **25** (1984), 339.

45.) *Intercalation Chemistry*, Americal Press. Inc. (1982) pp. 41, 46.

46.) N. Bartlett, E. M. McCarron and B. W. McQuillan, *Synth. Met.*, **1** (1979/80), 221.

47.) B. Zemva, K. Lutar, A. Jesih, W. J. Casteel, Jr. and N. Bartlett, submitted to *J. Chem. Soc., Chem. Comm.*, (1988).

48.) N. Bartlett and D. H. Lohmann, *Proc. Chem. Soc.*, **14** (1960), 115.

49.) N. Bartlett, *Proc. Chem. Soc.* (1962), 218.

50.) A. R. Young, T. Hirata and S. I. Morrow, *J. Amer. Chem. Soc.*, **86** (1964), 20.

51.) I. Solomon, R. I. Brabets, R. K. Uenishi, J. N. Keith and J. M. McDonough, *Inorg. Chem.*, **3** (1964), 457.

52.) J. Shamir and J. Binenboym, *Inorg. Chim. Acta.*, **2** (1968), 37.

53.) J. B. Beal, Jr., C. Pupp and W. E. White, *Inorg. Chem.*, **8** (1968), 828.

54.) K. Leary and N. Bartlett, *J. Chem. Soc., Chem. Comm.* (1972), 903.

55.) D. E. McKee and N. Bartlett, *Inorg. Chem.*, **12** (1973), 2738.

56.) A. J. Edwards, W. E. Falconer, J. E. Griffiths, W. A. Sunder and M. J. Vasile, *J. Chem. Soc. Dalton Tran.* (1974), **11**, 1129.

57.) M. J. Vasile and W. E. Falconer, *J. C. S. Dalton*, **4** (1975), 316.

58.) W. A. Sunder, A. E. Quinn and J. E. Griffiths, *J. Fluorine Chem.*, **6** (1975), 557.

59.) J. E. Griffiths, W. A. Sunder and W. E. Falconer, *Spectrochim. Acta.*, **31A** (1975), 1207.

60.) S. D. Brown, T. M. Loehr and G. L. Gard, *J. Fluorine Chem.*, **7** (1976), 19.

61.) K. O. Christe, R. D. Wilson and I. B. Goldberg, *Inorg. Chem.*, **15** (1976), 1271.

62.) N. B. S. (U. S. A.), Natl. Stand. Ref. Data Series NBS26 (1961), 151.

63.) P. A. Yeats and F. Aubke, *J. Fluorine Chem.*, **4** (1974), 243.

64.) A. Engelbrecht and A. V. Grosse, *J. Amer. Chem. Soc.*, **76**, 2042.

65.) T. J. Richardson, Ph.D. Thesis, University of California, Berkeley (1974).

66.) A. G. Streng and A. V. Grosse, *Advances in Chem.*, Ser. No. 36, A. C. S., Washington, D. C. (1962), 159.

67.) K. O. Christe, R. D. Wilson and I. B. Goldberg, *J. Fluorine Chem.*, **7** (1976), 543.

68.) A. G. Sharpe, *J. Chem. Soc. London* (1949), 2901.

69.) R. Hoppe and W. Klemm, *Z. Anorg. Allg. Chem.*, **268** (1952), 364.

70.) R. O. Peacock, *Chem. and Ind.* (1959), 904.

71.) A. J. Edwards and G. R. Jones, *J. Chem. Soc.* (1969), 1936.

72.) R. Hoppe, *Z. Anorg. Allg. Chem.*, **292** (1957), 28.

73.) R. Hoppe and R. Homann, *Z. Anorg. Allg. Chem.*, **379** (1970), 193.

74.) A. I. Popov, U. M. Kiselyev (1988).

75.) K. Lutar, A. Jesih and B. Zemva, *Revue de Chimie Minerale*, **23** (1986), 565.

76.) K. Lutar, A. Jesih, V. Leban and B. Zemva, submited to *J. Amer. Chem. Soc.* (1988).

77.) L. B. Asprey, K. H. Jack, H. Kruse and R. Maitland, *Inorg. Chem.*, **3** (1964), 602.

78.) F. W. B. Einstein, P. R. Trotter and N. Bartlett, *J. Chem. Soc.*, **A** (1967), 478.

79.) R. Bougon and M. Lance, *M. C. R. Seances Acad. Sci., Ser. 2*, **297** (1983), 117.

80.) R. Bougon, T. Bui Huy, M. Lance and H. Abazli, *Inorg. Chem.*, **23** (1984), 3667.

81.) N. Bartlett, unpublished result. Indexing was done on an X-ray powder photograph of AgF_3 prepared by B. Zemva and coworkers.

82.) Unpublished result obtained by D. Stewart working under N. Bartlett. Ag_9F_{16} and AgF_2 were identified and shown to possess characteristic X-ray powder patterns.

83.) C. G. Barraclough, J. Besida, P. G. Davies and T. A. O'Donnel, *J. Fluorine Chem.*, **38** (1988), 405.

84.) Result obtained by B. Zemva and reproduced in the present investigation.

85.) D. Stewart, unpublished result (1965).

86.) B. Zemva, W. J. Casteel, Jr., unpublished result.

87.) B. Cox, *J.*, (1956), 876.

88.) A. R. Young, II, T. Hirata and S. I. Morrow, *J. Amer. Chem. Soc.*, **86** (1964), 20.

89.) W. Jahn-Held and K. Jellinek, *Z. Elektrochem.*, **42** (1936), 608.

90.) A. Guntz, Guntz, *Bull. Soc. Chim. France*, **13(3)** (1895), 114.

91.) B. Zemva, W. J. Casteel, Jr., unpublished result.

92.) Swanson et al., NBS Circular, vol. V (1959), 539.

93.) B. Gruttner, M. F. A. Dove, A. F. Clifford, "Inorganic Chemistry in Liquid Hydrogen Cyanide and Liquid Hydrogen Fluoride" (1971), 177.

94.) J. A. McMillan, *J. Inorg. and Nucl. Chem.*, **13** (1960), 28.

95.) B. Frlec, D. Gantar and J. Holloway, *J. Fluorine Chem.*, **20** (1982), 217.

96.) B. Frlec, D. Gantar and J. Holloway, *J. Fluorine Chem.*, **20** (1982), 385.

97.) D. Gantar, B. Frlec, D. R. Russel and J. H. Holloway, *Acta. Cryst.*, **C43** (1987), 618.

98.) B. Zemva, private communication (1988).

ACKNOWLEDGEMENTS

I would like to thank Professor Neil Bartlett for his kind guidance and encouragement throughout the course of my graduate studies. His constant optimism and ability to untangle the most complex of problems was invaluable to the completion of my work.

I would also like to thank Tom Richardson for his instructive presence in the laboratory during my first few years, Ric Kaner for his help in the early stages of the boron nitride work, and Dino Kourtakis for his kind assistance in the laboratory and many helpful discussions. I am also grateful to Dr. Boris Zemva for his assistance in deciphering the silver (III) chemistry.

Finally, special thanks goes to the rest of the Bartlett group, Mike Lerner, John Kouvetakis, Rika Hagiwara, Bill Casteel, Byron Shen and Margrett Atkinson for the many good times, laughs, and *hope*ful conversations.

LAWRENCE BERKELEY LABORATORY
TECHNICAL INFORMATION DEPARTMENT
1 CYCLOTRON ROAD
BERKELEY, CALIFORNIA 94720